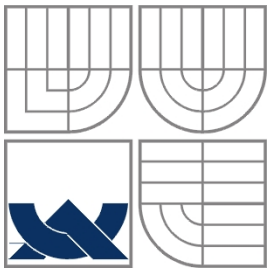


VYSOKÉ UČENÍ TECHNICKÉ V BRNĚ

BRNO UNIVERSITY OF TECHNOLOGY


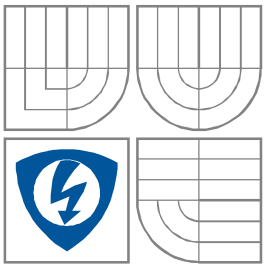


FAKULTA ELEKTROTECHNIKY A KOMUNIKAČNÍCH TECHNOLOGIÍ

ÚSTAV RADIOELEKTRONIKY

FACULTY OF ELECTRICAL ENGINEERING AND COMMUNICATION

DEPARTMENT OF RADIO ELECTRONICS


# HRANOVÉ KONEČNÉ PRVKY V ČASOVÉ OBLASTI

TIME DOMAIN EDGE FINITE ELEMENTS

DIPLOMOVÁ PRÁCE
MASTER'S PROJECT


AUTOR PRÁCE Bc. Jan Cigánek
AUTHOR

VEDOUCÍ PRÁCE prof. Dr. Ing. Zbyněk Raida
SUPERVISOR



BRNO, 2010

**VYSOKÉ UČENÍ TECHNICKÉ V BRNĚ**

**Fakulta elektrotechniky a komunikačních technologií**

**Ústav radioelektroniky**

# Diplomová práce

magisterský navazující studijní obor
**Elektronika a sdělovací technika**

***Student:*** Bc. Jan Cigánek ***ID:*** 78121
***Ročník:*** 2 ***Akademický rok:*** 2009/2010

**NÁZEV TÉMATU:**

## Hranové konečné prvky v časové oblasti

**POKYNY PRO VYPRACOVÁNÍ:**

Seznamte se s podstatou hybridních hranově-uzlových konečných prvků. Základní vlastnosti hybridních prvků ověřte jednoduchým programem pro modální analýzu planárních vedení.

Prostudujte různé přístupy k implementaci dokonale přizpůsobených vrstev. Vhodnou přizpůsobenou vrstvu použijte jako bezodrazové ukončení vlnovodu. Modelujte šíření harmonické vlny tímto vlnovodem (kmitočtová oblast).

Vytvořte verzi dokonale přizpůsobené vrstvy, kterou bude možné použít v časové oblasti. Modelujte šíření Gaussova impulzu tímto vlnovodem. Ve vlnovodu uvažujte systém štěrbin, kovových a dielektrických clonek. Sledujte chování struktury v časové a v kmitočtové oblasti.

**DOPORUČENÁ LITERATURA:**

[1] SILVESTER, P. P., FERRARI, R. F. Finite elements for electrical engineers. 3rd ed. Cambridge: Cambridge University Press, 1996.

[2] LEE, J. F., LEE, R., CANGELLARIS, R. Time domain finite element methods. IEEE Transactions on Antennas and Propagation. 1997, vol. 45, no. 3, p. 430-442.

***Termín zadání:*** 8.2.2010 ***Termín odevzdání:*** 21.5.2010

***Vedoucí práce:*** prof. Dr. Ing. Zbyněk Raida

**prof. Dr. Ing. Zbyněk Raida**
Předseda oborové rady

# LICENČNÍ SMLOUVA
# POSKYTOVANÁ K VÝKONU PRÁVA UŽÍT ŠKOLNÍ DÍLO

uzavřená mezi smluvními stranami:

**1. Pan/paní**

| | |
|---|---|
| Jméno a příjmení: | Bc. Jan Cigánek |
| Bytem: | Marefy 23, Bučovice, 685 01 |
| Narozen/a (datum a místo): | 16.dubna 1985 ve Vyškově |

(dále jen „autor“)

a

**2. Vysoké učení technické v Brně**

Fakulta elektrotechniky a komunikačních technologií
se sídlem Údolní 53, Brno, 602 00
jejímž jménem jedná na základě písemného pověření děkanem fakulty:
prof. Dr. Ing. Zbyněk Raida, předseda rady oboru Elektronika a sdělovací technika
(dále jen „nabyvatel“)

## Čl. 1

## Specifikace školního díla

1. Předmětem této smlouvy je vysokoškolská kvalifikační práce (VŠKP):

   ☐ disertační práce
   ☒ diplomová práce
   ☐ bakalářská práce
   ☐ jiná práce, jejíž druh je specifikován jako .....
   (dále jen VŠKP nebo dílo)

   | | |
   |---|---|
   | Název VŠKP: | Hranové konečné prvky v časové oblasti |
   | Vedoucí/ školitel VŠKP: | prof. Dr. Ing. Zbyněk Raida. |
   | Ústav: | Ústav radioelektroniky |
   | Datum obhajoby VŠKP: | _____ |

   VŠKP odevzdal autor nabyvateli*:

   ☒ v tištěné formě – počet exemplářů: 2
   ☒ v elektronické formě – počet exemplářů: 2

2. Autor prohlašuje, že vytvořil samostatnou vlastní tvůrčí činností dílo shora popsané a specifikované. Autor dále prohlašuje, že při zpracovávání díla se sám nedostal do rozporu s autorským zákonem a předpisy souvisejícími a že je dílo dílem původním.

3. Dílo je chráněno jako dílo dle autorského zákona v platném znění.

4. Autor potvrzuje, že listinná a elektronická verze díla je identická.

* hodící se zaškrtněte

## Článek 2

## Udělení licenčního oprávnění

1. Autor touto smlouvou poskytuje nabyvateli oprávnění (licenci) k výkonu práva uvedené dílo nevýdělečně užít, archivovat a zpřístupnit ke studijním, výukovým a výzkumným účelům včetně pořizovaní výpisů, opisů a rozmnoženin.

2. Licence je poskytována celosvětově, pro celou dobu trvání autorských a majetkových práv k dílu.

3. Autor souhlasí se zveřejněním díla v databázi přístupné v mezinárodní síti

   - ☒ ihned po uzavření této smlouvy
   - ☐ 1 rok po uzavření této smlouvy
   - ☐ 3 roky po uzavření této smlouvy
   - ☐ 5 let po uzavření této smlouvy
   - ☐ 10 let po uzavření této smlouvy

   (z důvodu utajení v něm obsažených informací)

4. Nevýdělečné zveřejňování díla nabyvatelem v souladu s ustanovením § 47b zákona č. 111/ 1998 Sb., v platném znění, nevyžaduje licenci a nabyvatel je k němu povinen a oprávněn ze zákona.

## Článek 3

## Závěrečná ustanovení

1. Smlouva je sepsána ve třech vyhotoveních s platností originálu, přičemž po jednom vyhotovení obdrží autor a nabyvatel, další vyhotovení je vloženo do VŠKP.

2. Vztahy mezi smluvními stranami vzniklé a neupravené touto smlouvou se řídí autorským zákonem, občanským zákoníkem, vysokoškolským zákonem, zákonem o archivnictví, v platném znění a popř. dalšími právními předpisy.

3. Licenční smlouva byla uzavřena na základě svobodné a pravé vůle smluvních stran, s plným porozuměním jejímu textu i důsledkům, nikoliv v tísni a za nápadně nevýhodných podmínek.

4. Licenční smlouva nabývá platnosti a účinnosti dnem jejího podpisu oběma smluvními stranami.

V Brně dne: 21. května 2010

…….. ……

Nabyvatel Autor

# ABSTRACT

This paper presents hybrid (edge and nodal) finite elements in frequency and time domain. The method is used for the numerical analysis of a parallel-plate waveguide loaded by two dielectric obstacles. A perfectly matched layer (PML) is implemented as the output port of this parallel-plate waveguide. In the project, the PLM layer for the exploitation in the time domain is developed. The method is programmed in MATLAB and is compared with results produced by COMSOL Multiphysics.

# KEYWORDS

Finite element method (FEM), hybrid finite elements, nodal finite elements, frequency domain, time domain, waveguide, perfectly matched layer (PML), MATLAB, COMSOL Multiphysics.

# ABSTRAKT

Diplomová práce se zabývá metodou hybridních (hranových a uzlových) konečných prvků ve frekvenční i časové oblasti. Tato metoda je použita pro analýzu vlnovodu *parallel-plate*, v kterém jsou umístěny dvě dielektrické vrstvy. Jako ukončení vlnovodu je implementována dokonale přizpůsobená vrstva označována PML. Projekt řeší možný výběr PML vrstvy v časové oblasti. Metoda je programována v programu MATLAB a výsledky jsou porovnány s programem COMSOL Multiphysics.

# KLÍČOVÁ SLOVA

Metoda konečných prvků, hybridní metoda konečných prvků, uzlová metoda konečných prvků, frekvenční oblast, časová oblast, vlnovod, dokonale přizpůsobená vrstva (PML), MATLAB, COMSOL Multiphysics.

CIGÁNEK, J. *Hranové konečné prvky v časové oblasti.* Brno: Vysoké učení technické v Brně, Fakulta elektrotechniky a komunikačních technologií, 2009. 40 s. Vedoucí diplomové práce prof. Dr. Ing. Zbyněk Raida.

# Prohlášení

Prohlašuji, že svou diplomovou práci na téma Hranové konečné prvky v časové oblasti jsem vypracoval samostatně pod vedením vedoucího diplomové práce a s použitím odborné literatury a dalších informačních zdrojů, které jsou všechny citovány v práci a uvedeny v seznamu literatury na konci práce.

Jako autor uvedené diplomové práce dále prohlašuji, že v souvislosti s vytvořením této diplomové práce jsem neporušil autorská práva třetích osob, zejména jsem nezasáhl nedovoleným způsobem do cizích autorských práv osobnostních a jsem si plně vědom následků porušení ustanovení § 11 a následujících autorského zákona č. 121/2000 Sb., včetně možných trestněprávních důsledků vyplývajících z ustanovení § 152 trestního zákona č. 140/1961 Sb.

V Brně dne 21. května 2010 .....

podpis autora

# Poděkování

Děkuji vedoucímu diplomové práce prof. Dr. Ing. Zbyňku Raidovi za účinnou metodickou, pedagogickou a odbornou pomoc a další cenné rady při zpracování mé diplomové práce.

V Brně dne 21. května 2010 .....

podpis autora

# Contents

# 1. Introduction

Hybrid finite elements can perform a proper simulation of electromagnetic fields. Using this method, a computation of physically non-existing solutions caused by an improper modeling of continuity boundary conditions can be eliminated [2], [8].

Finite elements are a differential numerical method which is able to handle with closed structures. In case of open structures, the solution space has to be truncated by proper boundary conditions. At present, perfectly matched layers are frequently used for this purpose [5], [9]. The perfectly matched layer (PML) is a nonphysical anisotropic lossy material, which behaves like a free space from the viewpoint of the propagating wave. Thanks to the losses, the wave is attenuated and zero boundary condition can be applied in the external surface of PML.

We have created a script in MATLAB, which can analyze a parallel-plate waveguide by hybrid finite elements in the time domain. The waveguide is loaded by two dielectric obstacles. The waveguide is terminated by a perfectly matched layer, which absorbs all the electromagnetic energy without reflections. This layer simulates free space.

# 2. Finite element method

The Finite Element Method (FEM) is an efficient numerical technique for solving Maxwell equations in the differential formulation. FEM can be applied directly on Maxwell equations or on wave equation. We will use the wave equation formulation. In [3], all important relations and derivations related to this topic were published [3], [4], [8].

Microwave structures can be analyzed by FEM in frequency domain or in time domain.

- Frequency domain finite elements (FDFE) can analyze electromagnetic field in the steady harmonic state.
- Time domain finite elements (TDFE) [4] are able to compute responses of structures to pulse excitations.

In the thesis, we will describe finite elements in both domains.

# 3. Hybrid finite elements

Hybrid finite elements are applied to provide a proper simulation tool for the computation of electromagnetic fields in environments containing various dielectrics of different parameters (permittivity and permeability) [2]. Thanks to hybrid finite elements, field continuity at the boundary of two dielectric sub-domains is properly modeled, and therefore, physically non-existing solutions are not produced.

Hybrid finite elements approximate longitudinal components of field intensity by nodal finite elements and transverse components of field intensity by edge elements. A detailed description of nodal finite elements and edge finite elements can be found in [2], [8].

In the thesis, we exploit a finite element formulation with identical matrices of coefficients both for the frequency domain and in the time domain. Therefore, the development of the frequency domain code can simplify the creation of the program in the time domain.

## 3.1 Frequency domain hybrid finite elements

The method is intended to solve full, non-simplified Maxwell equations [2]. In the approach adopted in this thesis, we use a final matrix equation for unknown nodal and edge approximation coefficients, which can be expressed for *n*-th finite element in the form [2]:

$$\begin{bmatrix} \mathbf{S}_t^{(n)} - k_0^2 \mu_r^{(n)} \tilde{\varepsilon}_r^{(n)} \mathbf{T}_t^{(n)} & 0 \\ 0 & \mathbf{S}_z^{(n)} - k_0^2 \mu_r^{(n)} \tilde{\varepsilon}_r^{(n)} \mathbf{T}_z^{(n)} \end{bmatrix} \begin{bmatrix} \mathbf{E}_t^{(n)} \\ \mathbf{E}_z^{(n)} \end{bmatrix} = \begin{bmatrix} 0 \\ 0 \end{bmatrix} \tag{3.1}$$

Here, $\mathbf{E}_t^{(n)}$ is the vector of the three unknown edge approximation coefficients, $\mathbf{E}_z^{(n)}$ is the vector of the three unknown nodal approximation coefficients, γ is the complex propagation constant, $k_0$ is the wave number in vacuum, $\mu_r^{(n)}$ is the relative permeability of *n*-th finite element, and $\tilde{\varepsilon}_r^{(n)}$ is the complex relative permittivity of *n*-th finite element.

Matrices $\mathbf{T}_t^{(n)}$, $\mathbf{S}_z^{(n)}$, $\mathbf{T}_z^{(n)}$ and $\mathbf{S}_t^{(n)}$ are matrices of finite-element coefficients of *n*-th finite element. Since the triangular finite element contains three edges and three vertices, the matrices are of the size $3 \times 3$ for linear basis functions [8].

The matrices can be evaluated using following relations [8]:

$$\mathbf{S}_t^{(n)} = \frac{1}{A^{(n)}} \begin{bmatrix} 1 & 1 & 1 \\ 1 & 1 & 1 \\ 1 & 1 & 1 \end{bmatrix}. \tag{3.2a}$$

$$\mathbf{T}_t^{(n)} = \frac{1}{12} \sum_{i=0}^{2} \mathbf{Q}_i \cot g\left[\theta_i^{(n)}\right]. \tag{3.2b}$$

$$\mathbf{S}_z^{(n)} = \frac{1}{2} \sum_{i=0}^{2} \mathbf{D}_i \cot g\left[\theta_i^{(n)}\right]. \tag{3.2c}$$

$$\mathbf{T}_z^{(n)} = \frac{A^{(n)}}{12} \begin{bmatrix} 2 & 1 & 1 \\ 1 & 2 & 1 \\ 1 & 1 & 2 \end{bmatrix}. \tag{3.2d}$$

Here

$$\mathbf{Q}_0 = \begin{bmatrix} 3 & -1 & -1 \\ -1 & 1 & 1 \\ -1 & 1 & 1 \end{bmatrix}, \qquad \mathbf{D}_0 = \begin{bmatrix} 0 & 0 & 0 \\ 0 & 1 & -1 \\ 0 & -1 & 1 \end{bmatrix}$$

$$\mathbf{Q}_1 = \begin{bmatrix} 1 & -1 & 1 \\ -1 & 3 & -1 \\ 1 & -1 & 1 \end{bmatrix}, \qquad \mathbf{D}_1 = \begin{bmatrix} 1 & 0 & -1 \\ 0 & 0 & 0 \\ -1 & 0 & 1 \end{bmatrix},$$

$$\mathbf{Q}_2 = \begin{bmatrix} 1 & 1 & -1 \\ 1 & 1 & -1 \\ -1 & -1 & 3 \end{bmatrix}, \qquad \mathbf{D}_2 = \begin{bmatrix} 1 & -1 & 0 \\ -1 & 1 & 0 \\ 0 & 0 & 0 \end{bmatrix}.$$

Next, $A^{(n)}$ is the area of *n*-th finite element and $\theta_i^{(n)}$ is the angle of the *i*-th vertex of the *n*-th finite element.

These relations are applied to the following form of the vector of nodal approximation coefficients ($e_z$) and edge approximation coefficients ($e_t$) [8]:

$$\mathbf{E}^{(n)} = \left[ e_{z,0}^{(n)} \quad e_{z,1}^{(n)} \quad e_{z,2}^{(n)} \quad e_{t,12}^{(n)} \quad e_{t,20}^{(n)} \quad e_{t,01}^{(n)} \right]^T . \tag{3.3}$$

## 3.2 Time domain hybrid finite elements

The simplest formulation of time-domain finite elements approximates the second order time derivative by a central difference [1]:

$$-k_0^2 \varphi = \mu_0 \varepsilon_0 \frac{d^2 \varphi}{dt^2} \approx \frac{1}{c^2} \frac{\varphi(i-1) - 2\varphi(i) + \varphi(i+1)}{\Delta t^2} . \tag{3.4}$$

Here, $c$ is the velocity of light, $\Delta t$ is the time step, $\varphi(i–1)$ is the time sample of a scalar function $\varphi$ in time $t = (i–1)\,\Delta t$, etc.

Reformulating the relation (3.1) for the time domain, we obtain [1]:

$$\left[ \frac{\varepsilon_r}{(c\Delta t)^2} \mathbf{T}_t \right] \mathbf{e}_t(i+1) = \left[ \frac{2\varepsilon_r}{(c\Delta t)^2} \mathbf{T}_t - \frac{1}{\mu_r} \mathbf{S}_t \right] \mathbf{e}_t(i) - \left[ \frac{\varepsilon_r}{(c\Delta t)^2} \mathbf{T}_t \right] \mathbf{e}_t(i-1) \tag{3.5a}$$

$$\left[ \frac{\varepsilon_r}{(c\Delta t)^2} \mathbf{T}_z \right] \mathbf{e}_z(i+1) = \left[ \frac{2\varepsilon_r}{(c\Delta t)^2} \mathbf{T}_z - \frac{1}{\mu_r} \mathbf{S}_z \right] \mathbf{e}_z(i) - \left[ \frac{\varepsilon_r}{(c\Delta t)^2} \mathbf{T}_z \right] \mathbf{e}_z(i-1) \tag{3.5b}$$

Equation (3.5) is an explicit algorithm. The matrices $\mathbf{S}_t$, $\mathbf{T}_t$ and $\mathbf{S}_z$, $\mathbf{T}_z$ are the same both for the frequency domain and for the time domain. This algorithm is less robust, and less universal than the implicit algorithm.

The implicit algorithm [1]:

$$\left[ \frac{\varepsilon_r}{(c\Delta t)^2} \mathbf{T}_t + \frac{1}{4\mu_r} \mathbf{S}_t \right] \mathbf{e}_t(i+1) = \left[ \frac{2\varepsilon_r}{(c\Delta t)^2} \mathbf{T}_t - \frac{1}{2\mu_r} \mathbf{S}_t \right] \mathbf{e}_t(i) - \left[ \frac{\varepsilon_r}{(c\Delta t)^2} \mathbf{T}_t + \frac{1}{4\mu_r} \mathbf{S}_t \right] \mathbf{e}_t(i-1) \tag{3.6a}$$

$$\left[ \frac{\varepsilon_r}{(c\Delta t)^2} \mathbf{T}_z + \frac{1}{4\mu_r} \mathbf{S}_z \right] \mathbf{e}_z(i+1) = \left[ \frac{2\varepsilon_r}{(c\Delta t)^2} \mathbf{T}_z - \frac{1}{2\mu_r} \mathbf{S}_z \right] \mathbf{e}_z(i) - \left[ \frac{\varepsilon_r}{(c\Delta t)^2} \mathbf{T}_z + \frac{1}{4\mu_r} \mathbf{S}_z \right] \mathbf{e}_z(i-1) \tag{3.6b}$$

is unconditionally stable. We will therefore use the implicit algorithm further.

## 3.3 Software implementation of edge finite elements

Software implementation of hybrid method finite elements is very similar to the implementation of nodal finite elements for the solution of quasi-static problems [2]. Therefore, we describe significant parts of code implementation only.

**Numbering of nodes and edges.** Local and global numbering of nodes is identical with numbering of nodes in pure nodal finite elements for the solution of quasi-static problems. Local edges are numbered as shown in Figure 3.1. In front of the zero local node, the zero local edge lies, etc. Global edges are numbered starting from the diagonal edge of the low-left element, and continuing by rows towards the top-right element. Horizontal and vertical edges are again numbered from the low-left element to the top-right one [2].

The way of numbering nodes and edges is up to the programmer.

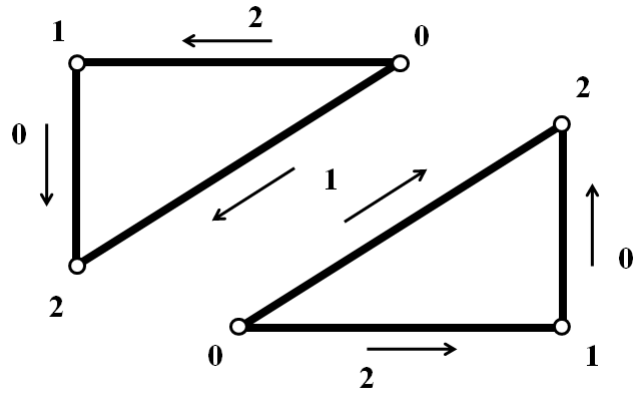


**Figure 3.1.** Local numbering of nodes and edges.

**Composition of matrix C**. This matrix joins local nodes and edges to global nodes and edges. The matrix **C** for nodes is identical with the finite-element code for the solution of quasi-static problems. The new matrix **C** for edges can contain two nonzero values in each column maximum (one or two edges contribute to a global edge). One of these nonzero values must be negative to express the different orientation of edge vectors [2].

**Boundary conditions**. We have to ensure that the tangential component of the intensity of electric field is zero at the perfect electric conductor (PEC)

$$\begin{aligned} \vec{n} \times \vec{E}_t &= \vec{0} \\ E_x &= 0 \end{aligned} \tag{3.7}$$

Here, $\vec{n}$ is unit vector normal to PEC, $\vec{E}_t$ is the transversal component of the electric field intensity vector and $E_x$ is the longitudinal component of the electric field intensity vector.

These conditions are implemented by removing those rows and columns from global matrices which can be found on perfect electric conductors.

Thanks to hybrid finite elements, field continuity at the boundary of two dielectric sub-domains is properly modeled, and therefore, physically non-existing solutions are not produced.

Results of the analysis and their comparison with the results produced by COMSOL Multiphysics are provided in Chapter 8.

# 4. Perfectly matched layers

A Perfectly matched layer (PML) is a nonphysical layer, which can absorb power of propagating electromagnetic wave without reflections. This feature allows modeling of open structures by differential methods like finite elements. In the thesis, PML is used to model an open-ended waveguide [5].

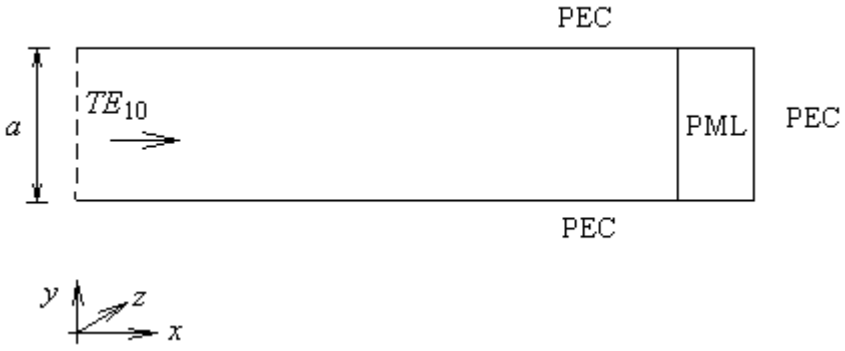


**Figure 4.1.** Parallel-plate waveguide terminated by PML layer.

Figure 4.1 shows a parallel-plate waveguide terminated by PML. The waveguide is excited by $TE_{10}$ mode. PML is implemented in the form of a two-dimensional (2-D) lossy material (uniaxial anisotropic lossy material) [5].

## 4.1 Frequency domain perfectly matched layer

Frequency domain PML adopted in this thesis has been described in [5]. Due to the anisotropic nature, PML is described by the frequency-dependent permittivity tensor

$$\overset{=p}{\varepsilon}_r = \varepsilon_r \begin{bmatrix} \dfrac{1}{1-j\dfrac{\sigma}{\omega\varepsilon_r\varepsilon_0}} & 0 & 0 \\ 0 & 1-j\dfrac{\sigma}{\omega\varepsilon_r\varepsilon_0} & 0 \\ 0 & 0 & 1-j\dfrac{\sigma}{\omega\varepsilon_r\varepsilon_0} \end{bmatrix},$$

where $\omega$ denotes angular frequency and $\sigma$ is conductivity

$$\sigma(x) = \frac{(m+1)\varepsilon_0\varepsilon_r c}{2d}\ln\left(\frac{1}{R}\right)\left(\frac{x-x_0}{d}\right)^m .$$

Here, $d$ is the depth of the PML, $m$ is the order of the spatial polynomial, $R$ is the desired reflection coefficient at normal incidence, and $x_0$ is the position of the PML interface.

Results of the analysis and their comparison with the results produced by COMSOL Multiphysics are provided in Chapter 6.

## 4.2 Time domain perfectly matched layer

Finite element method is applied to the solution of electric field vector wave equation. According to [5], we get the wave equation in frequency domain for transversal fields and longitudinal ones

$$\left(\nabla_t \times \mathbf{E}_t\right)\hat{\mu}_r^{-1}\left(\nabla_t \times \mathbf{E}_t\right)^* - k_0^2\left(\mathbf{E}_t\,\hat{\varepsilon}_r\,\mathbf{E}_t^*\right) = 0 , \tag{4.1}$$

$$\left(\nabla_t E_z\right)\hat{\mu}_r^{-1}\left(\nabla_t E_z^*\right) - k_0^2\left(E_z\,\hat{\varepsilon}_r\,E_z^*\right) = 0 . \tag{4.2}$$

Here, $\mathbf{E}_t = [E_x \;\; E_y]$ is the transversal component of the electric field, $E_z$ is the longitudinal component of the electric field, $\hat{\varepsilon}_r$ and $\hat{\mu}_r$ are permittivity and permeability tensors, respectively, $\varepsilon_0$ and $\mu_0$ are permittivity and permeability of vacuum, respectively, and $\nabla_t$ is the transverse operator.

$$\nabla_t = \begin{bmatrix} \frac{\partial}{\partial x} & \frac{\partial}{\partial y} \end{bmatrix}.$$

Finally, $k_0^2 = \omega^2 \mu_0 \varepsilon_0$ is the free space propagation constant and $\omega$ is angular frequency.

In the frequency domain, exploitation of hybrid finite elements converts (4.1) and (4.2) into the set of algebraic equations

$$\begin{bmatrix} \frac{1}{\mu_r}\mathbf{S}_t - k_0^2 \varepsilon_r \mathbf{T}_t & 0 \\ 0 & \frac{1}{\mu_r}\mathbf{S}_z - k_0^2 \varepsilon_r \mathbf{T}_z \end{bmatrix} \begin{bmatrix} \mathbf{e}_t \\ \mathbf{e}_z \end{bmatrix} = \begin{bmatrix} 0 \\ 0 \end{bmatrix} \tag{4.3}$$

In order to implement PML, $\varepsilon_r$ has to be a tensor

$$\hat{\varepsilon}_r = \begin{bmatrix} \varepsilon_{xx} & 0 & 0 \\ 0 & \varepsilon_{yy} & 0 \\ 0 & 0 & \varepsilon_{zz} \end{bmatrix} \tag{4.4}$$

Elements of the tensor are of the form, for example [9]

$$\varepsilon_{yy} = 1 - \frac{\sigma}{j\omega\varepsilon_0} \; . \tag{4.5}$$

Here, $j$ is complex unit.

In order to convert PML into the time-domain, central differences are applied:

$$-k_0^2 \varphi = \mu_0 \varepsilon_0 \frac{d^2\varphi}{dt^2} \approx \frac{1}{c^2} \frac{\varphi(i-1) - 2\varphi(i) + \varphi(i+1)}{\Delta t^2} \; , \tag{4.6}$$

where $c$ is the velocity of light, $\Delta t$ is the time step, $\varphi(i–1)$ is the time sample of a scalar function $\varphi$ in time $t = (i–1)\,\Delta t$, etc.

In time domain, PML coefficients have to be independent on angular frequency $\omega$. Obviously, we are not therefore able to derive an exact time-domain counterpart of PML.

We choose

$$\varepsilon_r = [I] + [\Sigma] \tag{4.7}$$

with

$$[I] = \begin{pmatrix} 1 & 0 & 0 \\ 0 & 1 & 0 \\ 0 & 0 & 1 \end{pmatrix} , \tag{4.8}$$

$$[\Sigma]=\begin{pmatrix} \frac{\sigma}{\varepsilon_0} & 0 & 0 \\ 0 & \frac{\sigma}{\varepsilon_0} & 0 \\ 0 & 0 & \frac{\sigma}{\varepsilon_0} \end{pmatrix}. \tag{4.9}$$

This choice enables us to rewrite (4.6) as

$$\begin{aligned} -k_0^2\varphi\varepsilon_r &= \mu_0\varepsilon_0\frac{d^2\varphi}{dt^2}[I]+\mu_0\varepsilon_0\frac{d\varphi}{dt}[\Sigma] \approx \\ &\approx \frac{1}{c^2}\left(\frac{\varphi(i-1)-2\varphi(i)+\varphi(i+1)}{\Delta t^2}[I]+\frac{\varphi(i-1)-\varphi(i+1)}{2\Delta t}[\Sigma]\right) \end{aligned} \tag{4.10}$$

resulting in

$$\begin{aligned} &\left[\frac{1}{(c\Delta t)^2}\mathbf{T}\left([I]+\frac{\Delta t}{2}[\Sigma]\right)\right]\mathbf{e}(i+1) = \\ &= \left[\frac{2}{(c\Delta t)^2}[I]\mathbf{T}-\frac{1}{\mu_r}\mathbf{S}[I]\right]\mathbf{e}(i)-\left[\frac{\varepsilon_r}{(c\Delta t)^2}\mathbf{T}\left([I]-\frac{\Delta t}{2}[\Sigma]\right)\right]\mathbf{e}(i-1) \end{aligned} \tag{4.11}$$

According to [10], the conductivity can be expressed in the following form:

$$\sigma(x)=\frac{\sigma_{max}\left|x-x_0\right|^m}{d^m}. \tag{4.12}$$

Here, $d$ is the depth of the PML, $x_0$ is the interface, and $m$ is the order of the polynomial variation. The maximum conductivity can be expressed as

$$\sigma_{max}=\frac{m+1}{150\pi h} \tag{4.13}$$

with $h$ being the spatial discretization (in meters).

A parallel-plate waveguide terminated by a PML was simulated in the time domain by MATLAB script. Figure 4.2 shows electromagnetic field distribution in the waveguide at the frequency 14 GHz.

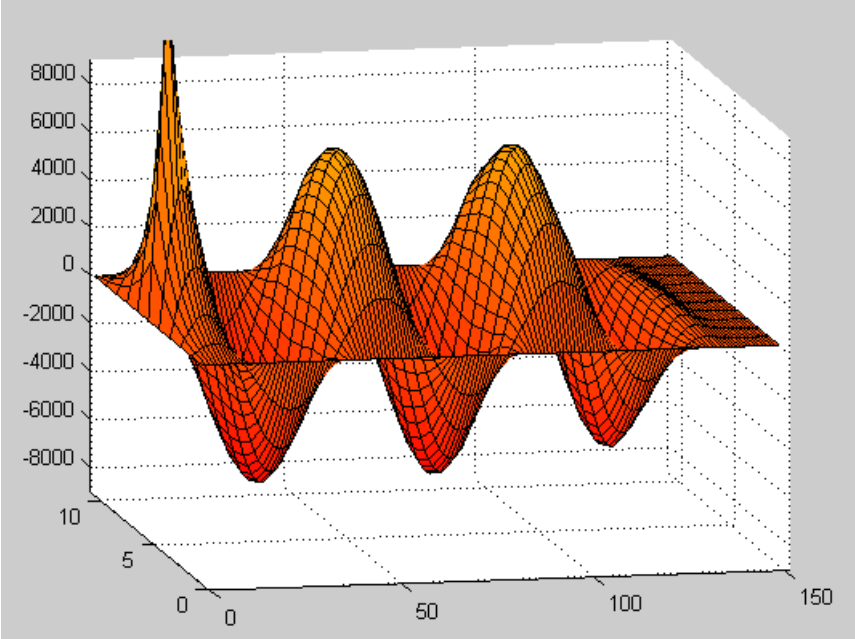


**Figure 4.2.** Distribution of the longitudinal component of electric field intensity in a parallel-plate waveguide terminated by PML in time domain.

Implementation of PML in the time-domain is easy. However, proper values of coefficients $d$, $m$, and $\sigma_{max}$ in (4.12) and (4.13) have to be set to obtain the required functionality. Moreover, optimum $\sigma(x)$ and the number of perfectly matched layers $N_x$ are also important for the simulation. A small number of perfectly matched layers $N_x$ and insufficient thickness of PML cause reflections. An optimum order of the polynomial variation has to be set according to the application.

The PML was implemented in the time domain finite element code as a uniaxial anisotropic lossy material. Comparison of results produced by our MATLAB program and computed by COMSOL Multiphysics shows good agreement.

# 5. Scattering parameters

Scattering parameters are used to characterize a microwave structures in frequency domain. At given frequency, $s_{11}$ corresponds to the reflection coefficient at the input of the structure, and $s_{12}$ describes transmission from the port 1 to the port 2.

In this project, we use scattering parameters for evaluating numerical reflections of a PML layer in frequency domain. For $N$-port planar devices, we get [11]

$$[\mathbf{Y}]_{mn} = \frac{-jb}{k_0 \eta_0} \left[\mathbf{E}^{(m)}\right]^T \left\{[\mathbf{S}] - k_0^2 [\mathbf{T}]\right\} \left[\mathbf{E}^{(n)}\right] \tag{5.1}$$

where $m$, $n$ = 1, …, $N$ and $N$ is the number of ports, $\eta_0$ is intrinsic impedance of free space, $b$ is the dimension of the structure in the direction of the translational symmetry, [$Y$] is the normalized admittance matrix for the device, $\mathrm{E}^{(k)}$ is the electric field intensity when there is a normalized voltage 1 V on port $k$ and all other ports are short-circuited. [S] and [T] are well-known global finite-element matrices.

The scattering matrix is given then by

$$[\mathbf{S}] = ([\mathbf{I_0}] + [\mathbf{Y}])^{-1}([\mathbf{I_0}] - [\mathbf{Y}]) \tag{5.2}$$

where $[\boldsymbol{I_0}]$ is the $N \times N$ identity matrix.

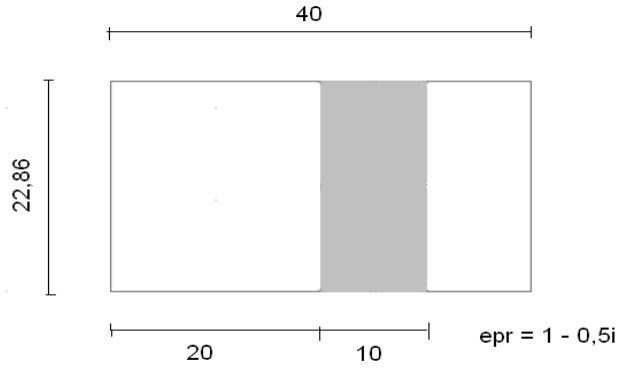


**Figure 5.1.** Testing structure for verifying calculations of scattering parameters.

In order to verify a proper computation of scattering parameters, we modeled the waveguide with a dielectric obstacle, which is terminated by the PEC wall (Figure 5.1). Results of the simulations (frequency response of scattering parameters) are depicted in Figure.5.2. The frequency response computed by the script is compared with results produced by COMSOL Multiphysics.

Differences between results are probably caused by different finite-element meshes used for computations. Further investigations are needed to confirm this hypothesis.

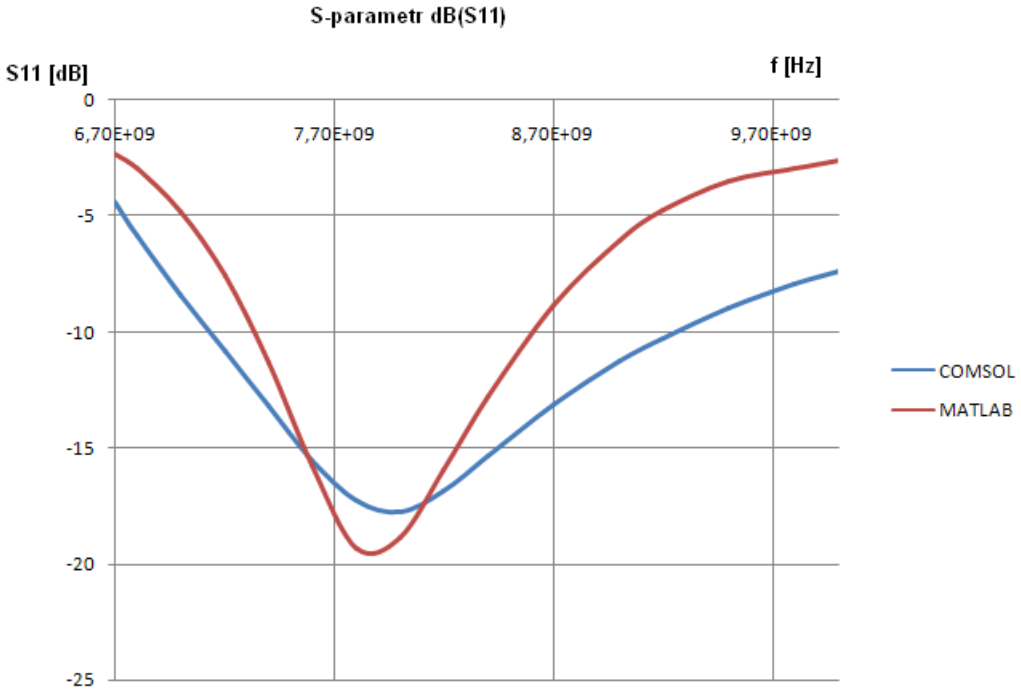


**Figure 5.2.** Frequency response of reflection coefficient at the input of the testing structure (blue – COMSOL, red – MATLAB).

# 6. Time domain characterization of PML

When testing numerical reflections of the PML termination, the backscattering coefficient (BC) [12] is determined. In order to evaluate numerical reflections in the time domain, FFT transform is used.

First, the parallel-plate waveguide is terminated by the PEC wall. This termination is used for reference. Second, the parallel-plate waveguide is terminated by PML layers. These terminations acquired in time-domain were transferred into frequency domain.

In order to determine BC, we use

$$BC(\omega) = \frac{FFT\{S_p(t) - S_s(t)\}}{FFT\{S_r(t) - S_s(t)\}} \tag{6.1}$$

where $S_p(t)$ is the signal when the waveguide is terminated by PML layers, $S_r(t)$ is the signal when the waveguide is terminated by the PEC wall, and $S_s(t)$ is the exciting signal.

The BC can be written in the logarithmic scale

$$BC_{dB} = 20\log(|BC|) \tag{6.2}$$

In order tor excite the waveguide, the Gaussian-modulated sinusoidal pulse with the defined center frequency and the fractional bandwidth is used (Figure 6.1).

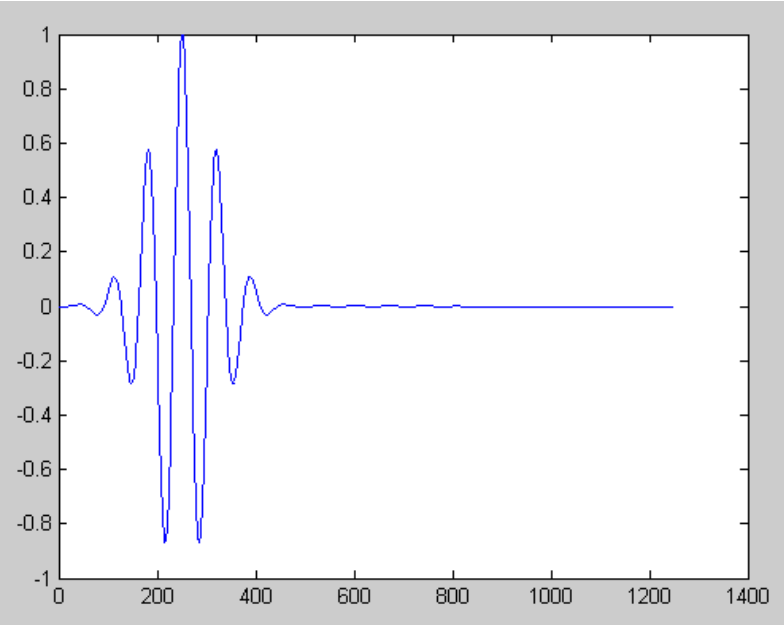


**Figure 6.1.** Exciting signal – Gaussian modulated sinusoidal pulse, center frequency is 14 GHz, fractional bandwidth is 0.4.

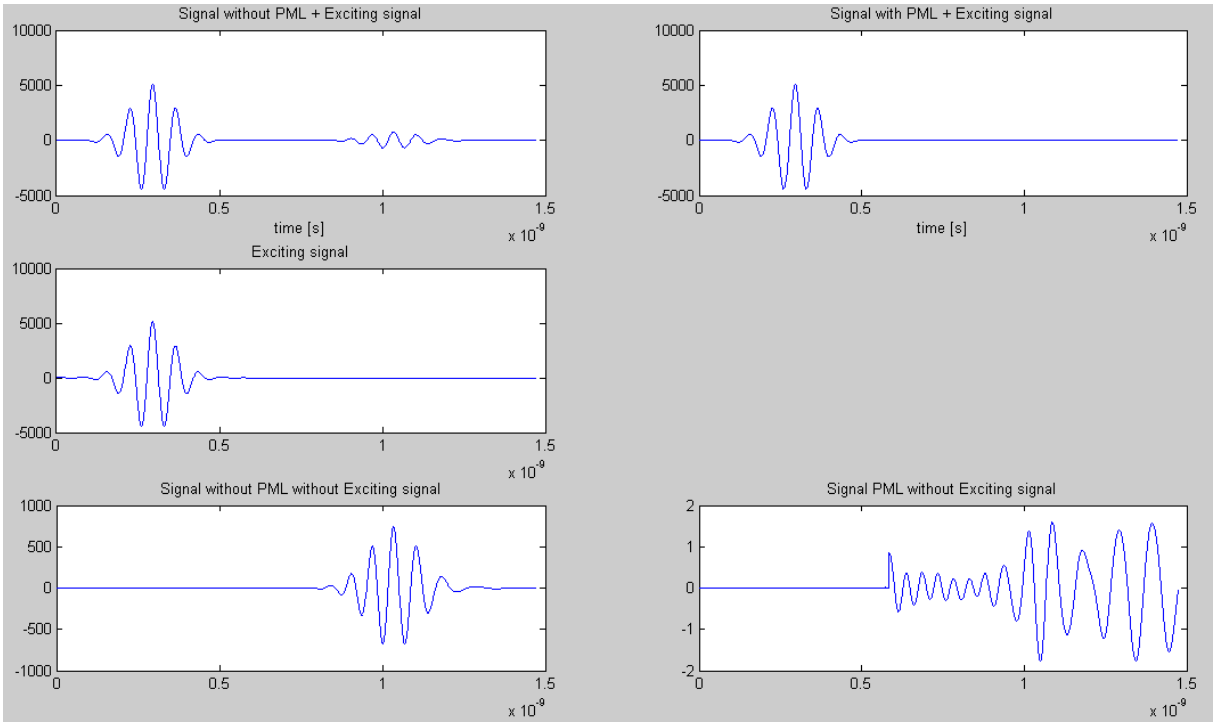


**Figure 6.2.** Signal of the parallel-plate waveguide terminated by the PEC wall (top left) and PML layers (top right). Exciting signal (center).
Signal of the parallel-plate waveguide without exciting signal terminated by the PEC wall (bottom left) and PML layers (bottom right).

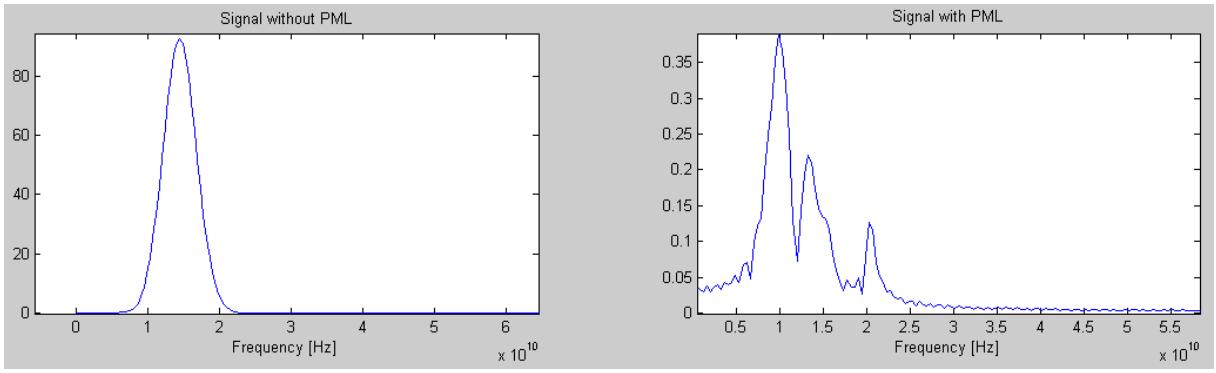


**Figure 6.3.** Spectrum of the parallel-plate waveguide terminated by the PEC (left) and PML layers (right).

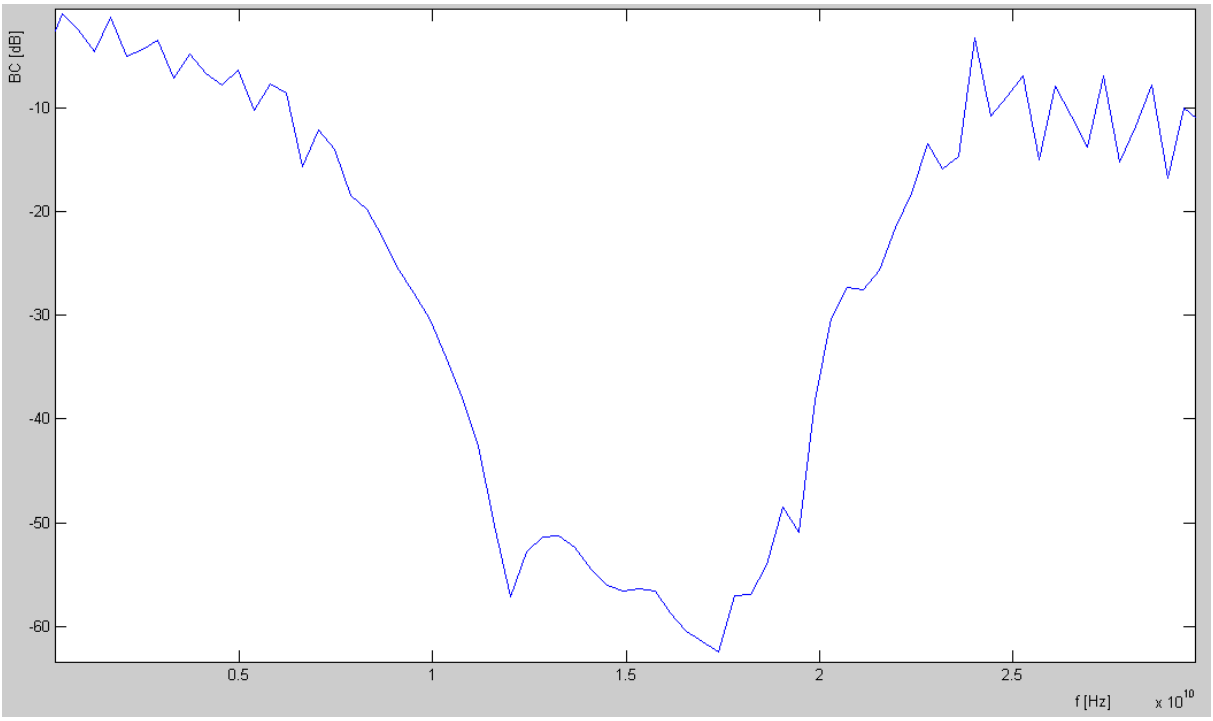


**Figure 6.4.** Calculated backscattering coefficient

Figure 6.4 shows frequency response of backscattering coefficient of the testing structure terminated by a PML layer. In a relatively wide frequency range, the backscattering coefficient achieves values as low as –50 dB. Further improvement of the perfectly matched layer can be achieved by changing the depth of the PML region, the number of layers, the mesh of finite elements, etc.

# 7. User's Guide

All programs are written in MATLAB. Programs allow modeling the propagation of electromagnetic waves in a waveguide. Programs implement the finite element method (FEM) both in the frequency domain and in the time domain.

Using PML, absorbing boundary condition at the end of the waveguide can be implemented. That way, the propagation of the forward wave without reflections can be modeled. This simulation mimics free space propagation of electromagnetic waves. The waveguide can be loaded by various dielectric obstacles.

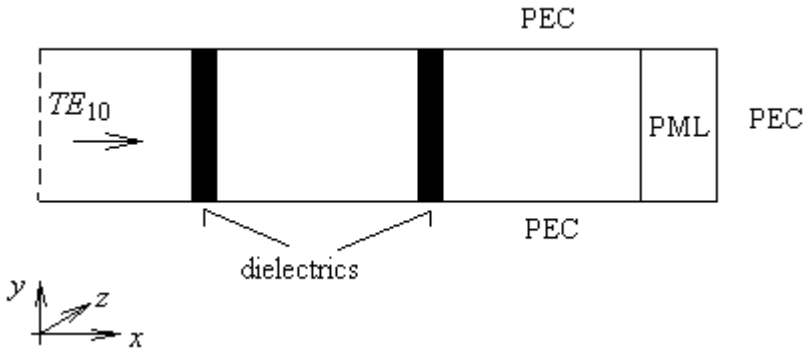


**Figure 7.1.** The model of the waveguide terminated by PML and loaded by dielectric obstacles.

In Figure 7.1, *x* is the axis oriented to the direction of wave propagation, PML denotes the perfectly matched layer and PEC is perfect electric conductor.

## 7.1 Frequency Domain + PML

The program is based on frequency domain finite elements and frequency domain PML consisting of 6 layers. The program is run from the Command Window of MATLAB by typing:

```
main( Nx, Ny, dx, dy, epr1, epr2, i1, i2, w1, w2, f )
```

Here:

| | |
|---|---|
| `Nx` | number of elements in x-axis |
| `Ny` | number of elements in y-axis |
| `dx` | longitudinal dimension of waveguide [mm] |
| `dy` | transversal dimension of waveguide [mm] |
| `epr1` | relative permittivity of dielectric obstacle 1 |
| `epr2` | relative permittivity of dielectric obstacle 2 |
| `i1` | coordinate of left surface of dielectric obstacle 1 [mm] |
| `i2` | coordinate of left surface of dielectric obstacle 2 [mm] |
| `w1` | width of dielectric obstacle 1 [mm] |
| `w2` | width of dielectric obstacle 2 [mm] |
| `f` | frequency [GHz] |

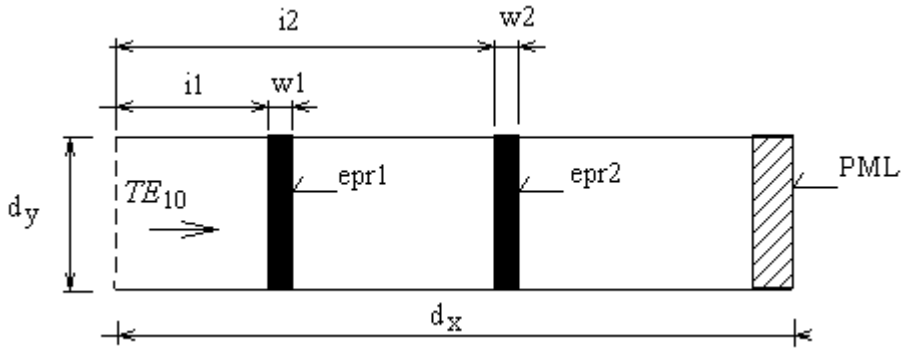


**Figure 7.2.** Explanation of parameters of the frequency domain program.

Let us model the following structure. The waveguide is divided into Nx = 150 and Ny = 10 rectangular elements. The length of the waveguide is dx = 80 mm, and the height of the waveguide equals to dy = 22.86 mm. The first obstacle is of relative permittivity equal to 9, of the left coordinate 20 mm and the width is 10 mm. The second obstacle is of the relative permittivity equal to 9, of the left coordinate 50 mm and the width is 10 mm. The frequency is 14 GHz. The corresponding command is:

```
main( 150, 10, 80.00, 22.86, 9, 9, 20, 50, 10, 10, 14 )
```

resulting into the field distribution depicted in Figure 7.3.

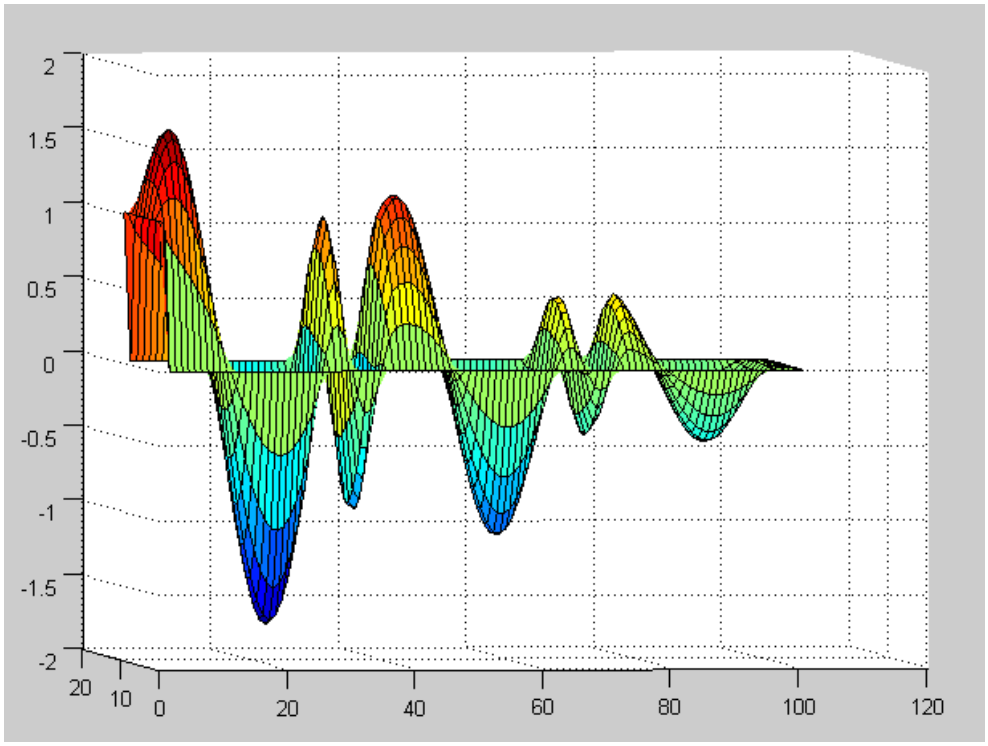


**Figure 7.3.** Distribution of the longitudinal component of electric field intensity in the waveguide loaded by two dielectric obstacles and terminated by PML. Frequency domain.

## 7.2 Time Domain + PML

The program can be run from the Command Window of MATLAB by typing:

```
main( Nx, Ny, dx, dy, epr1, epr2, i1, i2, w1, w2,  PML, f)
```

Here:

| | |
|---|---|
| `Nx` | number of elements in x-axis |
| `Ny` | number of elements in y-axis |
| `dx` | longitudinal dimension of waveguide [mm] |
| `dy` | transversal dimension of waveguide [mm] |
| `epr1` | relative permittivity of dielectric obstacle 1 |
| `epr2` | relative permittivity of dielectric obstacle 2 |
| `i1` | coordinate of left surface of dielectric obstacle 1 [mm] |
| `i2` | coordinate of left surface of dielectric obstacle 2 [mm] |
| `w1` | width of dielectric obstacle 1 [mm] |

`w2` width of dielectric obstacle 2 [mm]
`PML` the number of elements of PML layer (PML = 0 for waveguide without PML)
`f` frequency [GHz]

Let us model the following structure. The waveguide is divided into Nx = 150 and Ny = 10 rectangular elements. The length of the waveguide is dx = 80 mm, and the height of the waveguide equals to dy = 22.86 mm. The first obstacle is of relative permittivity equal to 9, of the left coordinate 20 mm and the width is 10 mm. The second obstacle is of the relative permittivity equal to 9, of the left coordinate 50 mm and the width is 10 mm. The number of PML elements is 100. The corresponding command is:

```
main(150, 10, 80.00, 22.86, 9, 9, 20, 50, 10, 10, 100, 14 )
```

resulting into the field distribution depicted in Figure 7.4.

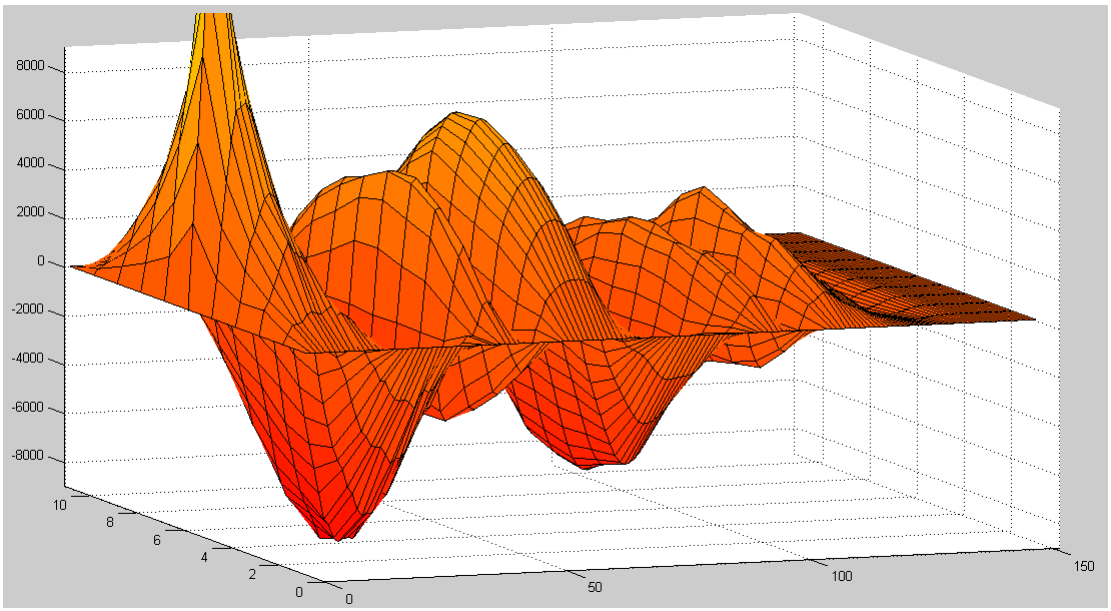


**Figure 7.4.** Distribution of the longitudinal component of electric field intensity in the waveguide loaded by two dielectric obstacles and terminated by PML. Time domain.

# 8. Results of simulations

In this chapter, we will model a parallel-plate waveguide loaded by two dielectric obstacles and terminated by a PML (see Figure 8.1). However, the PML can be set according to the application. The results are compared with COMSOL Multiphysics.

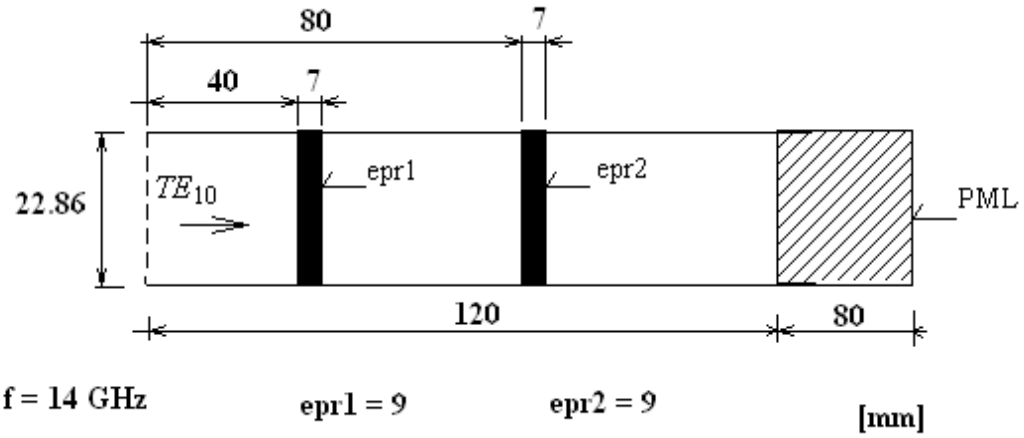


**Figure 8.1.** Parallel-plate waveguide loaded by dielectric obstacles and terminated by PML to be analyzed by the developed MATLAB scripts.

## 8.1 Frequency domain

We are going to model the waveguide depicted in Figure 8.1. This waveguide is terminated by the perfect electric conductor. In this model, standing waves appear between the excitation wall, the dielectric obstacles and the end of the waveguide.

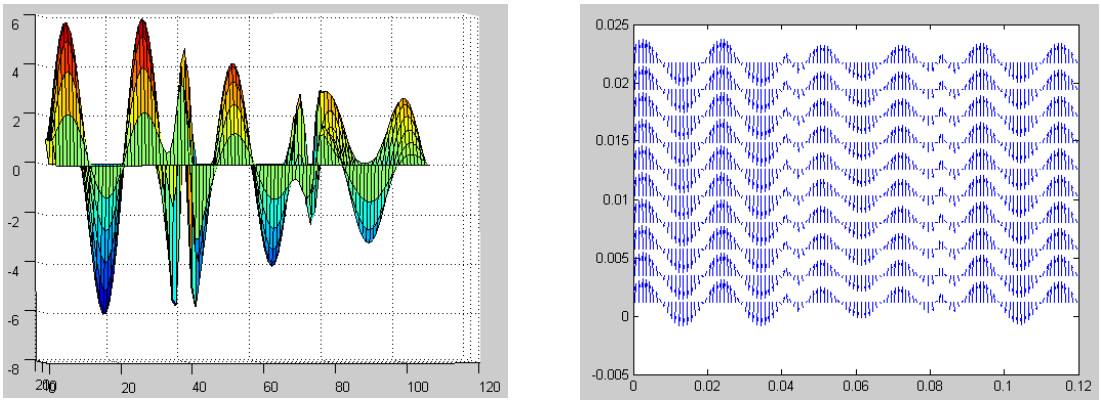


**Figure 8.2.** Results provided by the MATLAB script analyzing the waveguide from Figure 8.1. The waveguide is terminated by the PEC wall. Left: the distribution of the longitudinal component of electric field intensity. Right: the distribution of the transversal vectors of electric field intensity in the parallel-plate waveguide.

In the second numerical study, we use a PML to terminate the waveguide (Figure 8.3.). The perfectly matched termination influences fields in the waveguide section between the second dielectric obstacle and the end of the waveguide. In this section, the forward wave is absorbed in PML, and no electromagnetic energy is reflected back.

PML in the frequency-domain was implemented according to the Chapter 4.1 and 7.1 [5]. We can use PML consisting of a small number layers (6 to 10 layers). Then, the reflection coefficient at the normal incidence is $R = 10^{-4}$ and the order of the spatial polynomial equals to $m = 2$. In Figures 6.3 and 6.4, the depth of the used PML is 15 mm. This model was created according to [5].

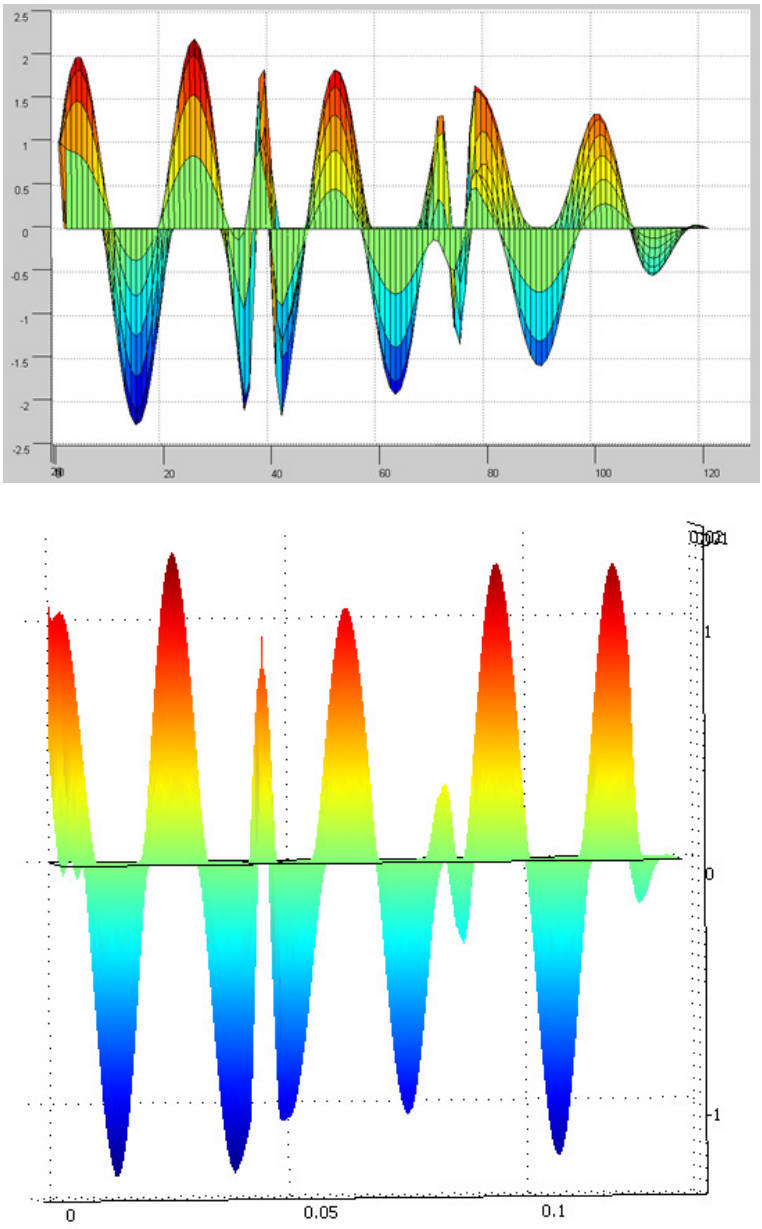


**Figure 8.3.** Distribution of the longitudinal component of electric field intensity in the parallel-plate waveguide depicted in Figure 6.1. Top: results provided by MATLAB script. Bottom: results provided by COMSOL Multiphysics.

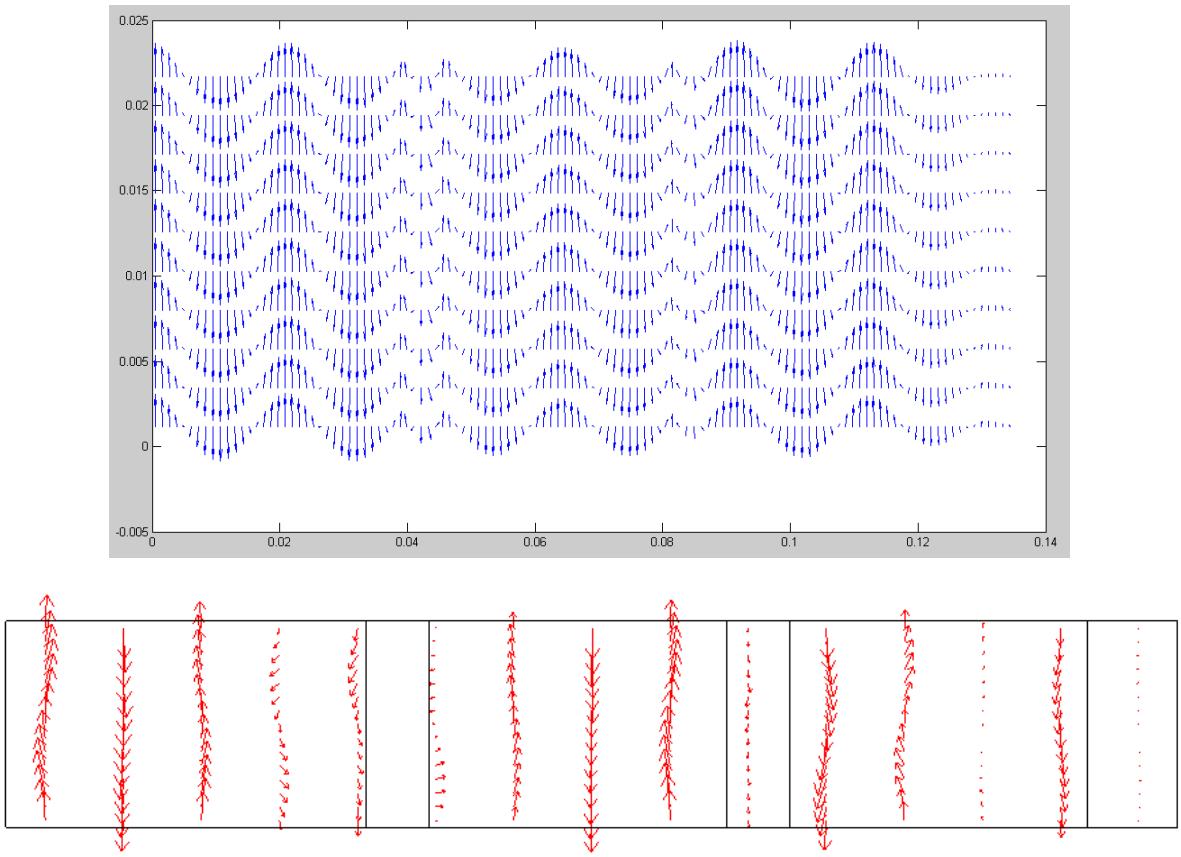


**Figure 8.4.** Distribution of the transversal vectors of electric field intensity in the parallel-plate waveguide depicted in Figure 8.1. Top: results provided by MATLAB script. Bottom: results provided by COMSOL Multiphysics.

## 8.2 Time domain

First, we model the waveguide depicted in Figure 8.1. The waveguide is terminated by perfect electric conductor. In this model, standing waves appear between the excitation wall, the dielectric obstacles and the end of the waveguide.

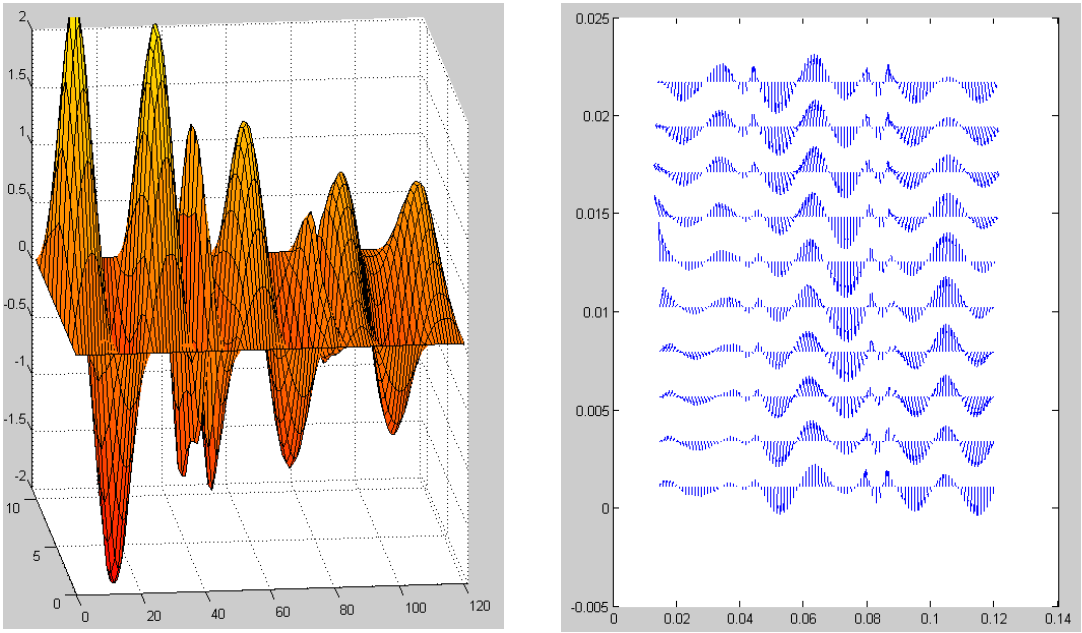


**Figure 8.5.** Results provided by the MATLAB script analyzing the waveguide from Figure 8.1. The waveguide is terminated by the PEC wall. Left: the distribution of the longitudinal component of electric field intensity. Right: the distribution of the transversal vectors of electric field intensity in the parallel-plate waveguide.

In the second numerical study, we use a PML to terminate the waveguide (Figure 8.6.). The perfectly matched termination influences fields in the waveguide section between the second dielectric obstacle and the end of the waveguide. In this section, the forward wave is absorbed in PML, and no electromagnetic energy is reflected back.

PML in the time-domain was implemented according to the Chapter 4.2 and 7.2. We can use PML consisting of a large number layers (80 layers). The order of the spatial polynomial equals to $m$ = 13. In Figures 8.6 and 8.7, the depth of the used PML is 80 mm. This model did not cause any reflections.

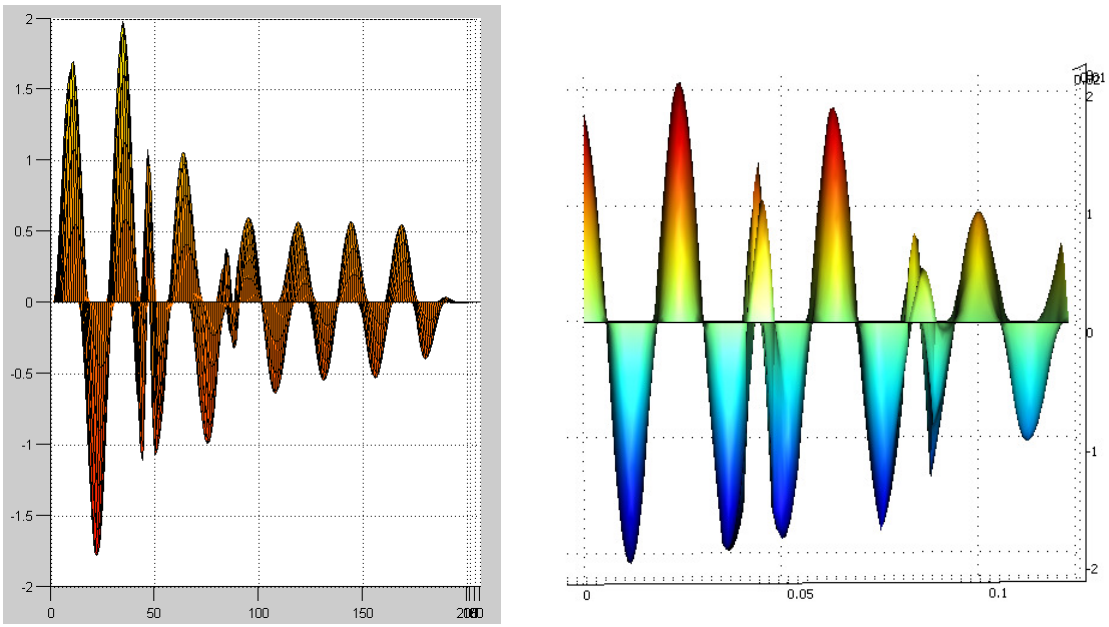


**Figure 8.6.** Distribution of the longitudinal component of electric field intensity in the parallel-plate waveguide depicted in Figure 8.1. Left: results provided by MATLAB script. Right: results provided by COMSOL Multiphysics.

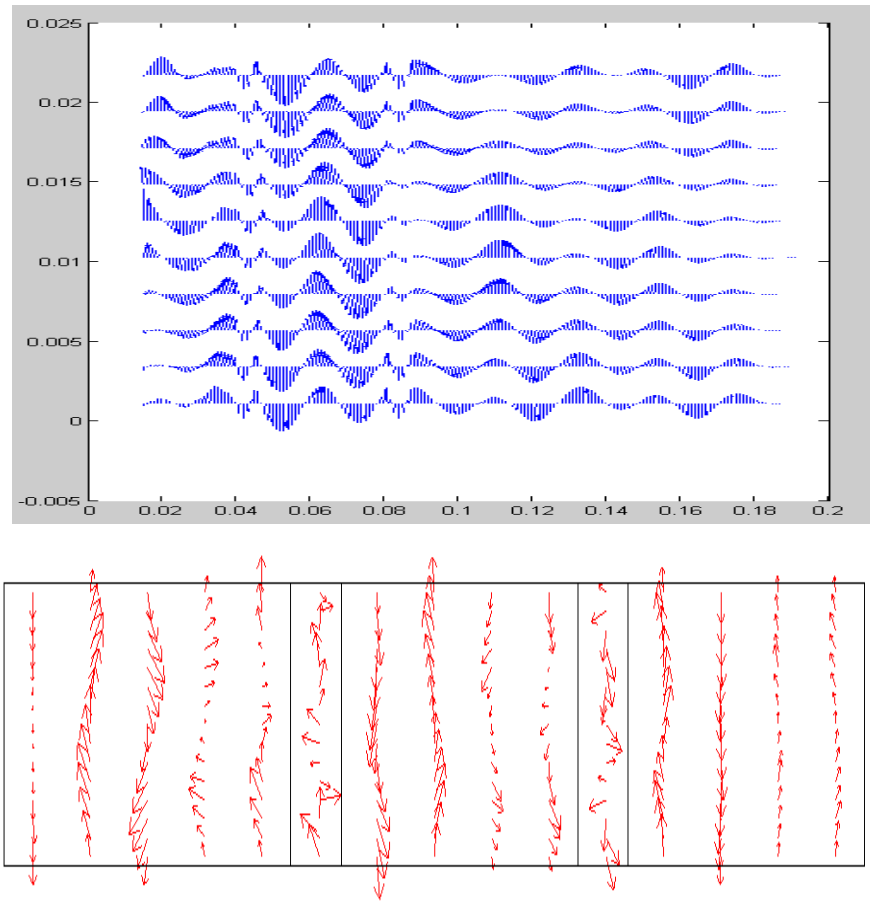


**Figure 8.7.** Distribution of the transversal vectors of electric field intensity in the parallel-plate waveguide depicted in Figure 8.1. Top: results provided by MATLAB script. Bottom: results provided by COMSOL Multiphysics.

## 8.3 Frequency domain PML

In this chapter, we investigate the influence of the finite-element mesh on characteristics of the PML in frequency domain. As a reference, results produced by COMSOL Multiphysics are considered.

The model of the waveguide (Figure 8.8) was terminated by a four-layer PML medium of the total depth 20 mm. The PML was created according to [5] with the desired reflection coefficient at normal incidence $10^{-4}$ and the order of the spatial polynomial 2. The waveguide was excited by the $TE_1$ mode. We used four different discretization meshes. The reflection coefficient [20 log($S_{11}$)] as a function frequency is depicted in Fig. 8.10.

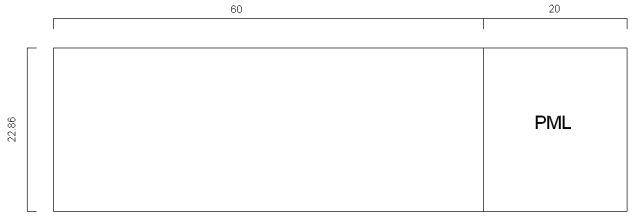


**Figure 8.8.** Model of waveguide.

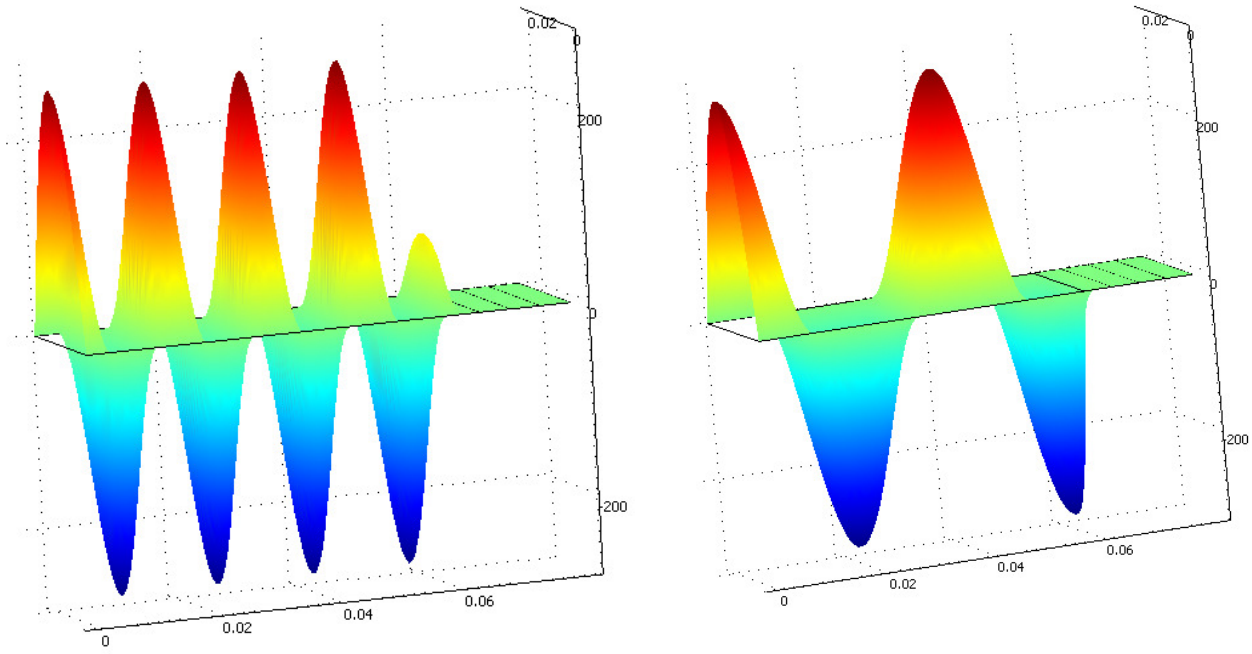


**Figure 8.9.** Left: Result of simulation $f = 20$ GHz. Right: Result of simulation $f = 10$ GHz.

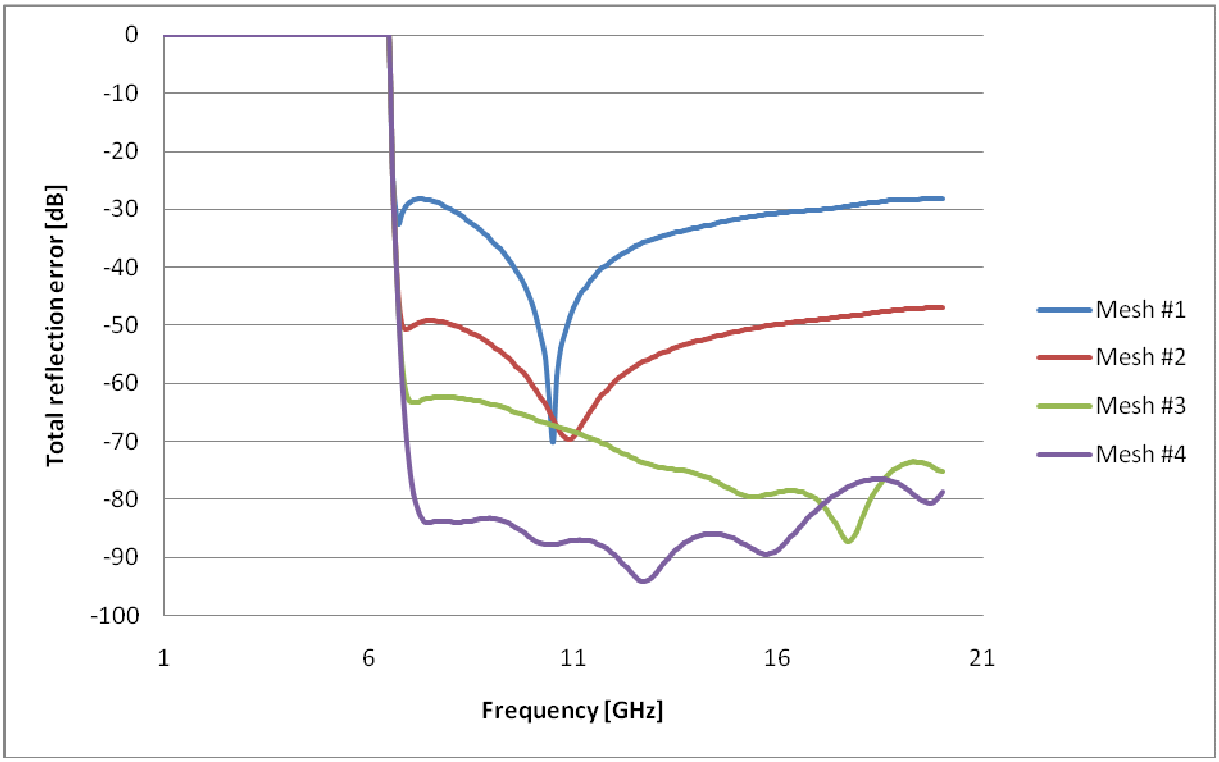


**Figure 8.10.** The reflection coefficient as a function of frequency (COMSOL).

We used meshes with the following number of elements.

Elements in PML:

Mesh #1 – 80 elements
Mesh #2 – 320 elements
Mesh #3 – 1100 elements
Mesh #4 – 4100 elements

The PML was analyzed over a wide frequency range. A reflection error was different for every mesh. With the increased number of elements, the reflection error is decreasing.

When analyzing the testing structure in MATLAB, results of simulations in form of the reflection coefficient [20 log($S_{11}$)] are depicted as a function of frequency in Figure 8.11.

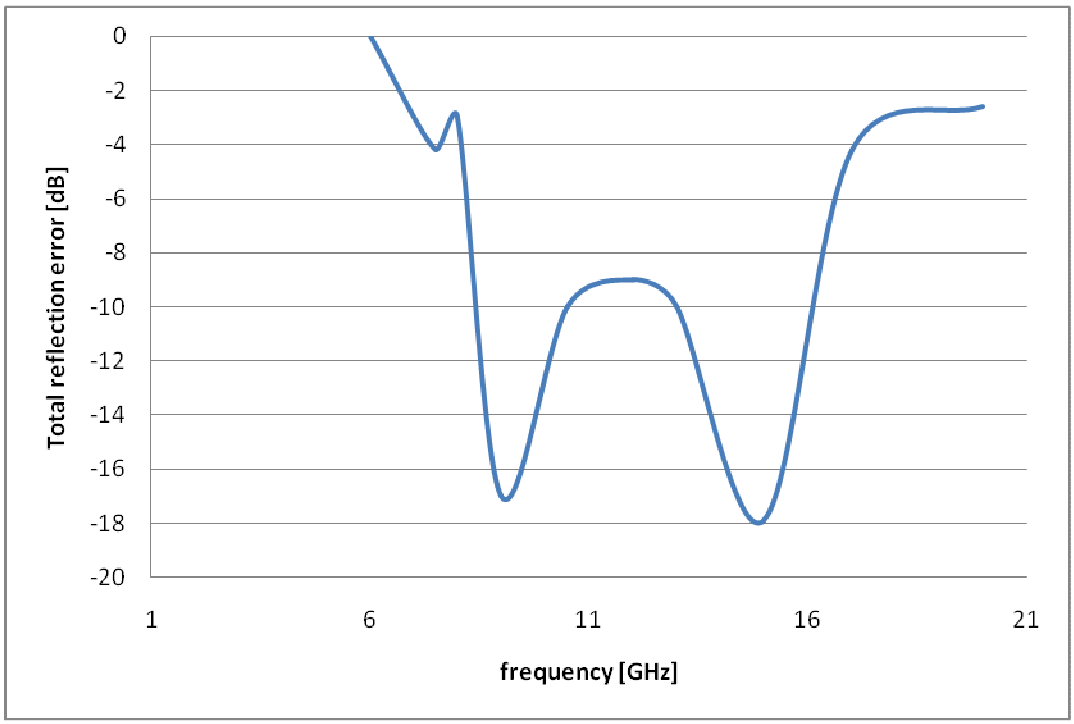


**Figure 8.11.** The reflection coefficient as a function frequency (MATLAB)

We can see that the reflection coefficient does not reach such values like simulations in COMSOL. The problem is caused by the used mesh of finite elements (simple rectangular triangles in case of MATLAB program).

## 8.4 Time domain PML

We search a waveguide terminated by the PEC wall which meets the scattering boundary condition: $E_{0x} = 0$, $E_{0y} = 0$, $E_{0z} = 0$. In Figure 8.12, the waveguide model with the described boundaries is depicted.

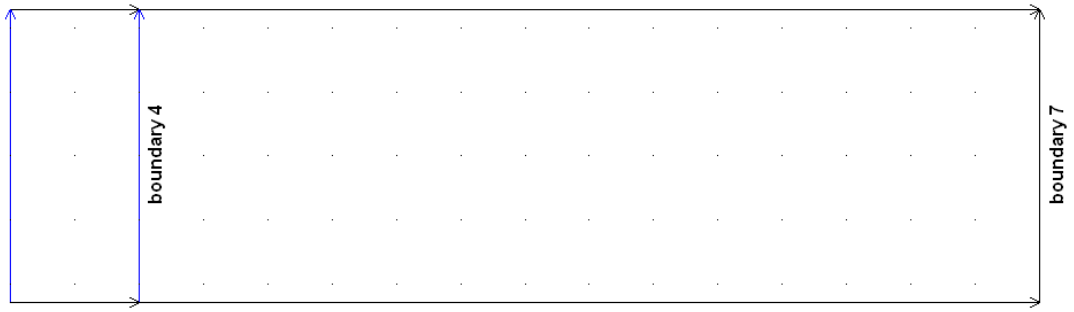


**Figure 8.12.** Waveguide, boundary 4 is the integration boundary.

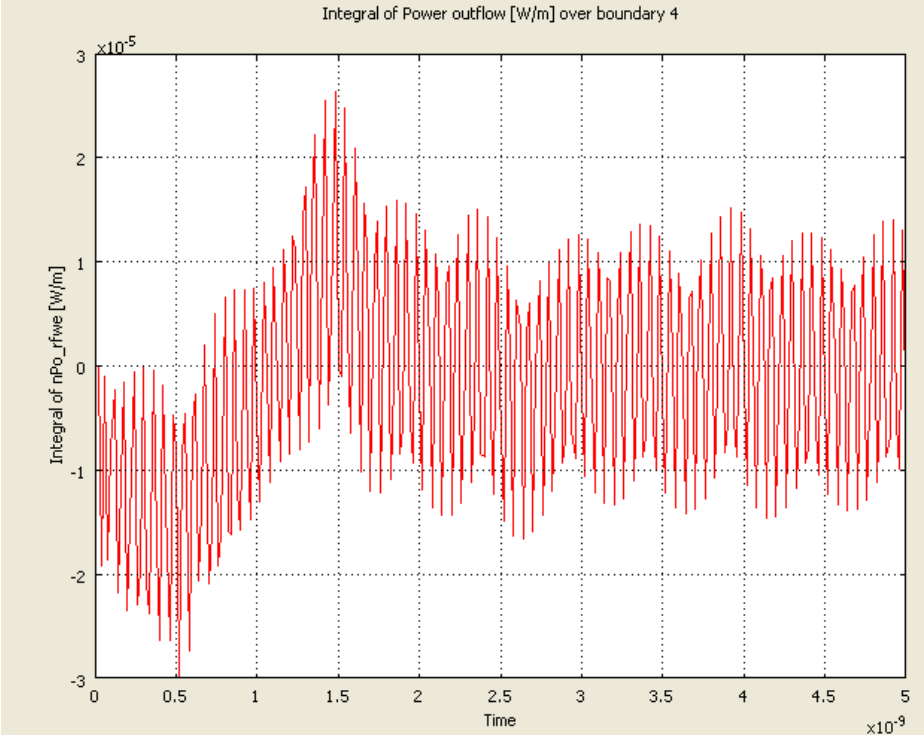


**Figure 8.13.** Integral of power outflow over boundary 4 from Figure 8.12; boundary 7 is perfect electric conductor.

The integral of the power outflow over the boundary 4, where the boundary 7 is perfect electric conductor, is depicted in Figure 8.13. First, the power outflow is less then zero. The energy is propagating from the excitation wall to the boundary 7. Second, the power outflow is greater than zero. The energy is propagating from the boundary 7 to the excitation wall. Finally, standing waves appear in the waveguide between the excitation wall and the boundary 7.

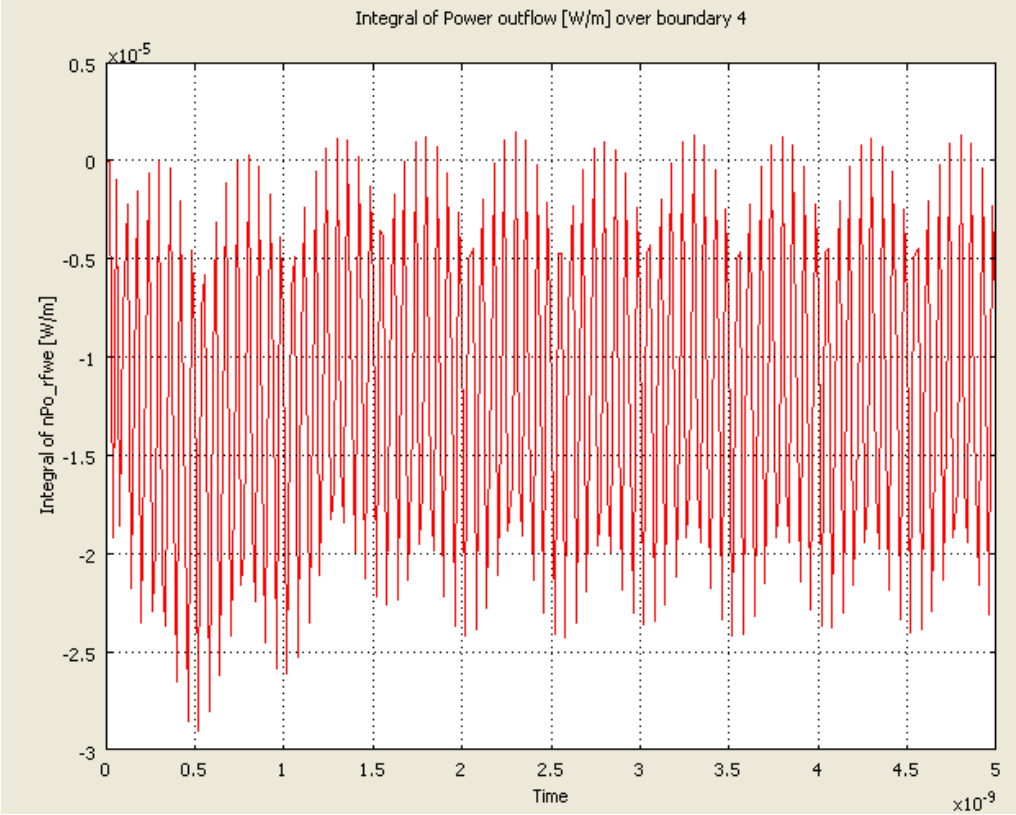


**Figure 8.14.** Integral of power outflow over boundary 4 from Figure 8.12; boundary 7 is adjusted as scattering boundary condition: $E_{0x} = 0$, $E_{0y} = 0$, $E_{0z} = 0$.

The integral of the power outflow over the boundary 4, when the boundary 7 is adjusted as the scattering boundary condition $E_{0x} = 0$, $E_{0y} = 0$, $E_{0z} = 0$, is depicted in Figure 8.14. The power outflow is less then zero. The energy is propagating from the excitation wall to the boundary 7.

Now, the calculations are repeated using the MATLAB script. We use the PML layer created in the previous chapter, and we analyze the model of the waveguide depicted in Figure 8.12. As the exciting signal, the harmonic signal (Figures 8.15 and 8.16) and the Gaussian-modulated sinusoidal pulse (Figures 8.17 and 8.18) are used.

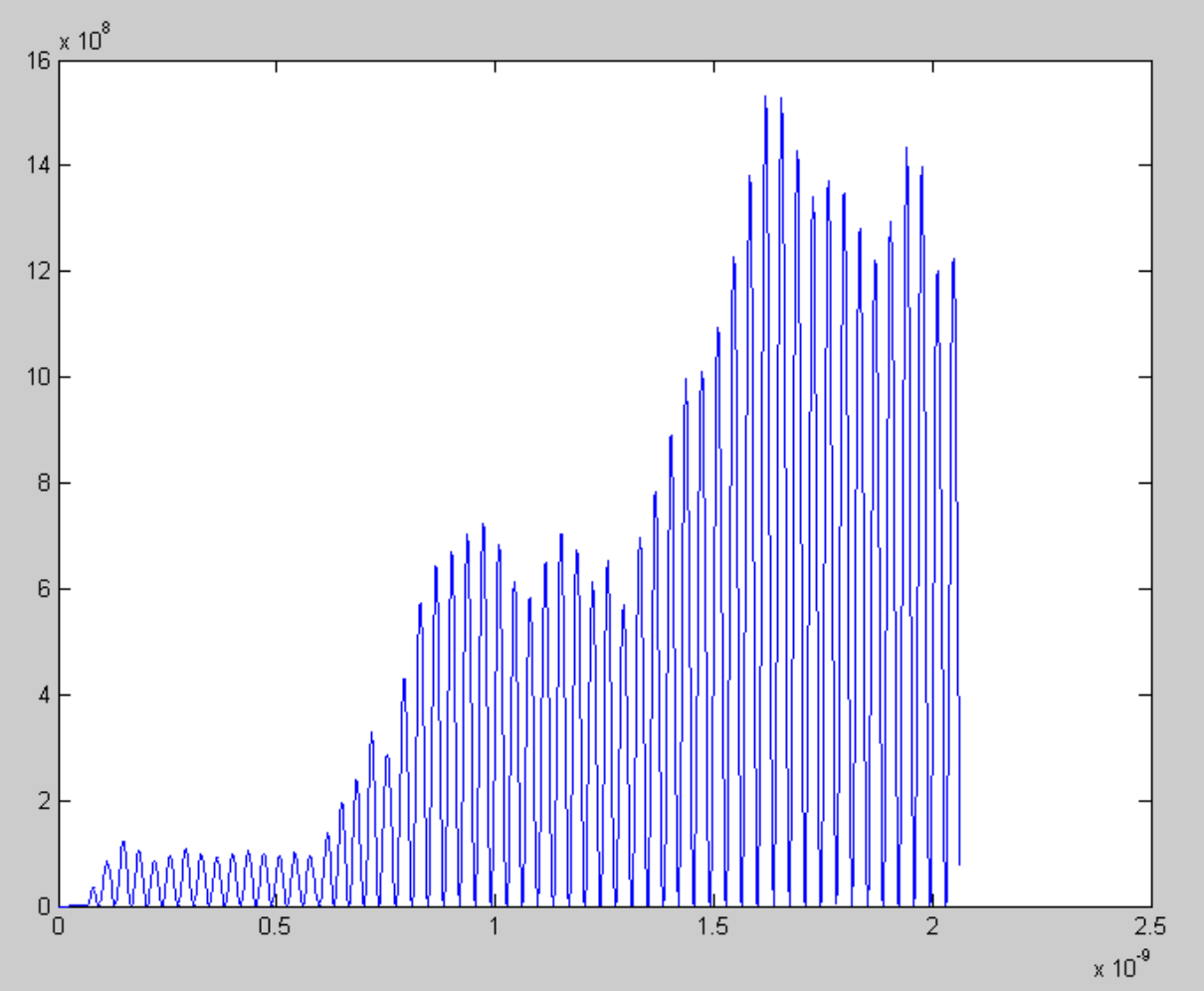


**Figure 8.15.** Integral of power outflow over boundary 4 from Figure 8.12, boundary 7 is perfect electric conductor. Harmonic exciting signal is used.

The integral of the power outflow over the boundary 4, when the boundary 7 is perfect electric conductor, is depicted in Figure 8.15. The exciting signal is the harmonic signal. We can see that the power outflow is growing in time. In the waveguide, standing waves appear between the excitation wall and the boundary 7.

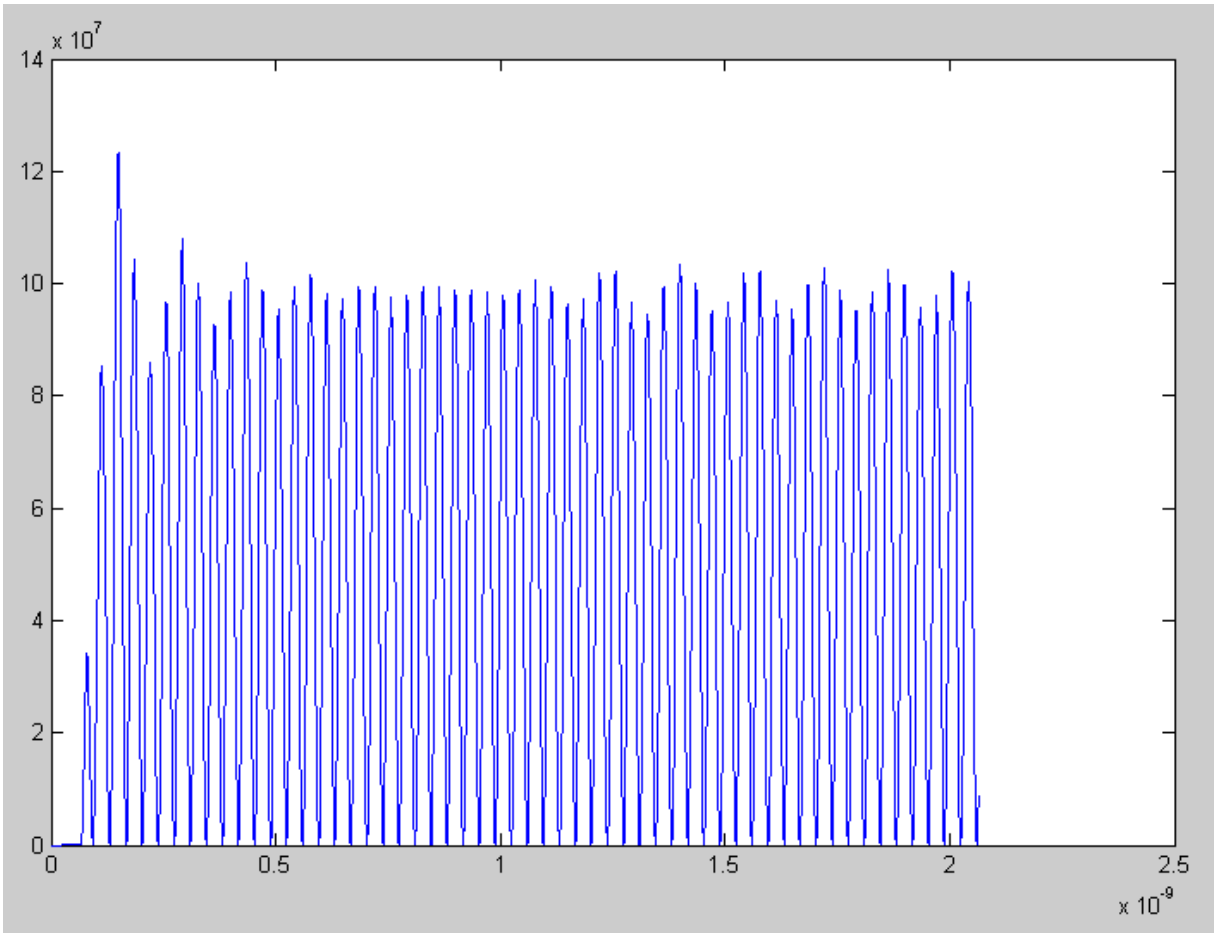


**Figure 8.16.** Integral of power outflow over boundary 4 from Figure 8.12; boundary 7 is replaced by PML layer. Harmonic exciting signal is used.

The integral of the power outflow over the boundary 4, where the boundary 7 is replaced by the PML layer, is depicted in Figure 8.16. Harmonic exciting signal is used. We can see no growth of the power outflow in time. In the waveguide, no standing waves are formed.

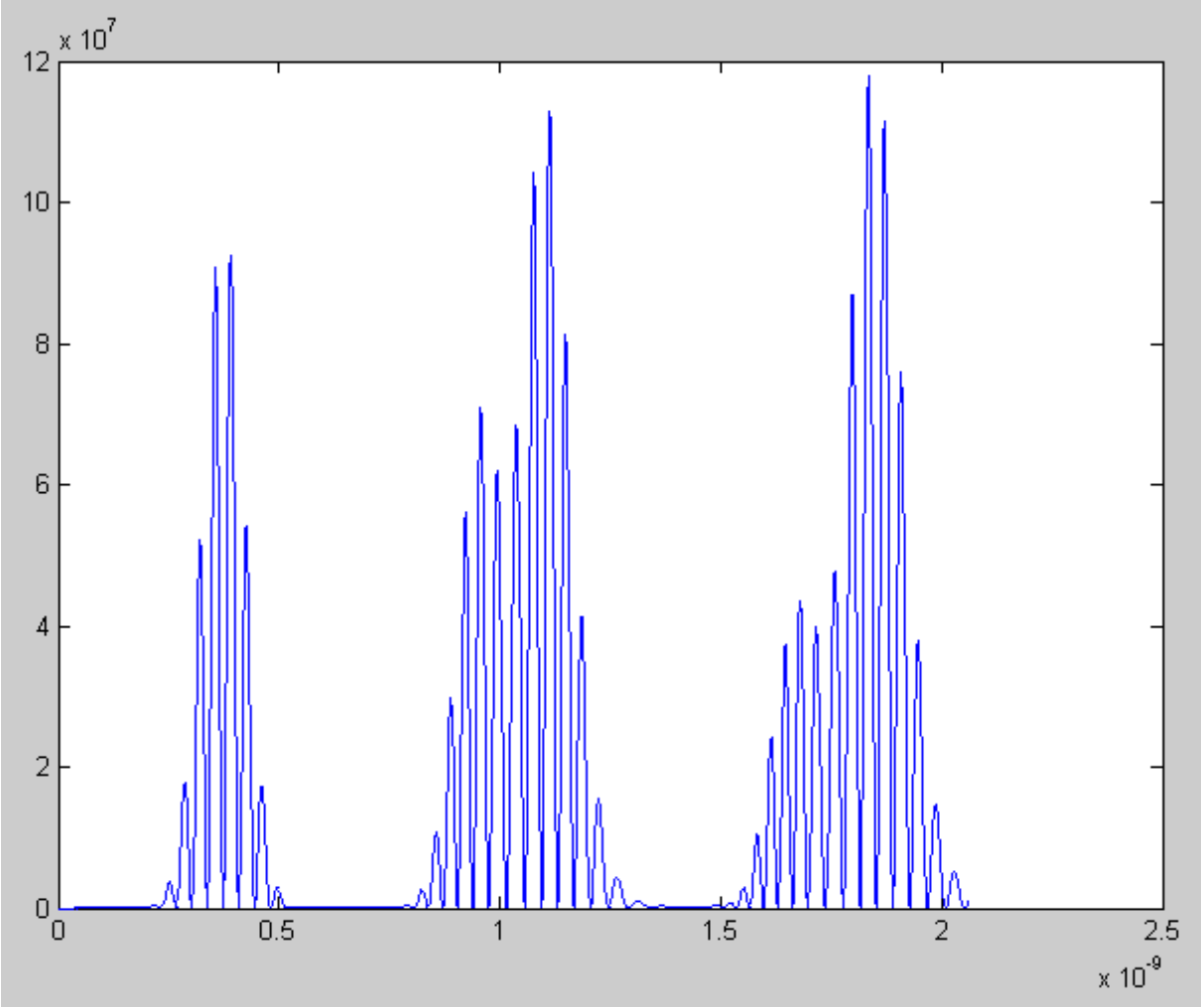


**Figure 8.17.** Integral of power outflow over boundary 4 from Figure 8.12; boundary 7 is perfect electric conductor. Exciting Gaussian-modulated sinusoidal pulse is used.

The integral of the power outflow over the boundary 4, where the boundary 7 is perfect electric conductor, is depicted in Figure 8.17. Exciting Gaussian-modulated sinusoidal pulse is used. We can see growing power outflow in time. In the waveguide, one pulse between the excitation wall and the boundary 7 is propagating.

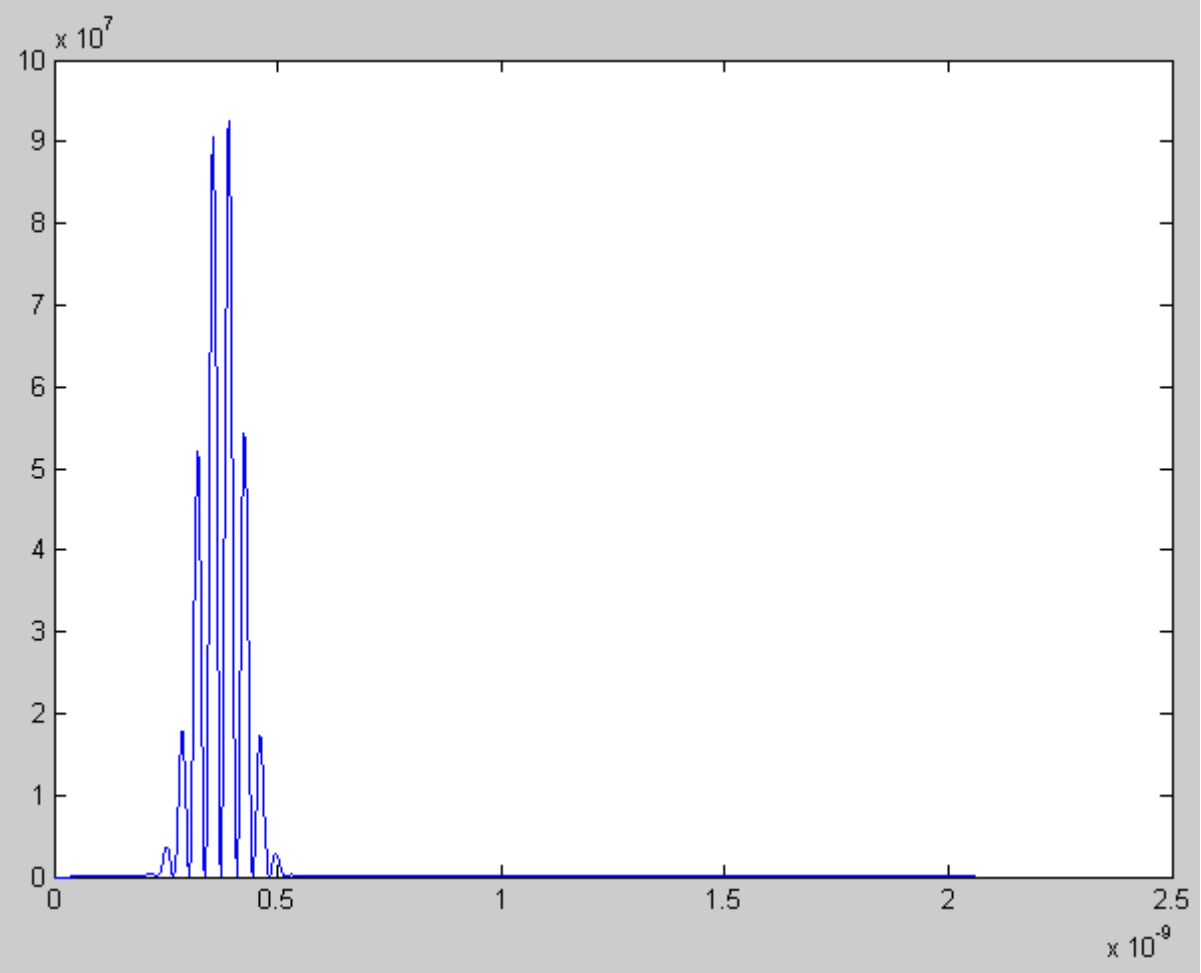


**Figure 8.18.** Integral of power outflow over boundary 4 from Figure 8.12; boundary 7 is replaced PML layer. Exciting signal is Gaussian-modulated sinusoidal pulse.

The integral of the power outflow over the boundary 4, where the boundary 7 is replaced by the PML layer, is depicted in Figure 8.18. Exciting Gaussian-modulated sinusoidal pulse is used. We can see that there is no growing power outflow in time. In the waveguide, no standing waves are formed.

# 9. Conclusions

In the project, a MATLAB script for the finite element analysis of a parallel-plate waveguide loaded by dielectric obstacles was developed for frequency domain and time domain. The waveguide can be terminated by a perfectly matched layer, which absorbs all the electromagnetic energy without reflections. All the results have been validated using COMSOL Multiphysics.

Parameters (numerical reflections) of the created frequency-domain PML strongly depend on the quality of the mesh of finite elements over a wide range of frequencies for simulations carried out in COMSOL Multiphysics. Properties of the developed frequency-domain PML were evaluated by calculating the scattering parameter S11.

If the frequency-domain PML is simulated in MATLAB, significantly worse results are obtained: the MATLAB code exploits a simple mesh consisting of rectangular finite elements,

which negative influences the results. Achievement of better results is conditioned by using a high-quality mesh.

The PML was also implemented in a 2-D finite element formulation in the time domain. The PML was evaluated by integrating the power outflow. In COMSOL Multiphysics, the waveguide was terminated by the PEC wall which meets the scattering boundary condition: $E_{0x} = 0$, $E_{0y} = 0$, $E_{0z} = 0$. Calculated integrals are given by appropriate figures. In MATLAB, we used the harmonic signal and the Gaussian-modulated sinusoidal pulse as the excitation signal. Calculated integrals are also given by appropriate figures. Using the backscattering coefficient, the values lower than –50 dB were achieved in a relatively wide range of frequencies. The developed time-domain PML was used for a simple mesh consisting of rectangular triangles.

# 10. References


[1] RAIDA, Z. a kol. *Analýza mikrovlnných struktur v časové oblasti*. Brno: Nakladatelství VUTIUM, 2004.

[2] RAIDA, Z.; ČERNOHORSKÝ, D.; NOVÁČEK, Z.; ŠKVOR, Z. *Analýza a optimalizace mikrovlnných struktur.* Brno: Nakladatelství VUTIUM, 1999.

[3] SILVESTER, P. P.; FERRARI, R. L. *Finite Elements for Electrical Engineers*. 3rd Edition. Cambridge: Cambridge University Press, 1996.

[4] LEE, J. F.; LEE, R.; CANGELLARIS, R. Time domain finite element methods. *IEEE Transactions on Antennas and Propagation*, 1997, vol. 45, no. 3, p. 430–442.

[5] POLYCARPOU, C.; LYONS, M. R. A two-dimensional finite element formulation of the perfectly matched layer. *IEEE Microwave and Guided Wave Letters*, 1996, vol. 6, no. 9, p. 338–340.

[6] *COMSOL Multiphysics Help* [počítačový program]. Ver. 3.3.0.405. Stockholm (Sweden): COMSOL A.G., 2006.

[7] *MATLAB Help* [počítačový program]. Ver. 7.1.0.246 (R14) SP3. Natick (USA): Mathworks, 2005.

[8] RAIDA, Z. a kol. *Multimediální učebnice elektromagnetických vln a mikrovlnné techniky*. Internetová učebnice. Brno: FEKT VUT v Brně, 2001.

[9] TAFLOVE, A.; HAGNESS, A. *Computational Electrodynamics: the finite-difference time-domain method*. 2nd Edition. Norwood: Artech House, 2003.

[10] MATHIS, V. An anisotropic perfectly matched layer-absorbing medium in finite element time domain method for Maxwell's equations. In *Proceedings of the International Symposium of IEEE Antennas and Propagation Society*, 1997, p. 680 to 683.

[11] GARCIA, P.; WEBB, J.P. *Optimization of Planar Devices by the Finite Element Method. IEEE Transactions on microwave theory and techniques*, 1990, vol. 38, no. 1, p. 48–53.

[12] YHANG, J.; HUANG, Y. *Extraction of dielectric properties of building materials from free-space time-domain measurement. IEEE High frequency postgraduate student colloquium*, 1999.

# 11. List of figures

# 12. List of symbols

| | |
|---|---|
| **E** | Electric field intensity |
| $\mathbf{E}_t$ | Transverzal component of the electric field |
| $E_z$ | Longitudial component of the electric field |
| $\omega$ | Angular frequency |
| $k_0$ | Free space propagation constant |
| $\mu_0$ | Permeability of vacuum |
| $\varepsilon_0$ | Permittivity of vacuum |
| $\mu_r$ | Relative permeability |
| $\varepsilon_r$ | Relative permittivity |
| $\sigma$ | Electric conductivity |
| TE | Transverse electric wave |
| BC | Backscattering coefficient |
| $\bar{S}$ and $\bar{T}$ | Matrices of finite-element coefficient |
| PEC | Perfect electric conductor |
| PML | Perfectly matched layer |
| FFT | Fast Furier transform |
| S11 | Reflection coefficient |
| $c$ | Velocity of light |
| $\Delta t$ | time step |
| $\vec{n}$ | unit vector normal |
| $m$ | Order of the spatial polynomial |
| $\nabla_t$ | Transverse operator |
| $\eta_0$ | Intrinsic impedance of free space |